EVALUATION OF IMMOBILIZATION PROTOCOLS OF A FLUORESCENCE-BASED IMMUNOSENSOR USED TO DETECT INFECTIOUS DISEASES

by

Wisanu Simalai

A Thesis Submitted in Partial Fulfillment of the Requirements for the Degree of Master of Engineering in Nanotechnology

Examination Committee:	Dr. Raffaele Ricco (Chairperson)
	Dr. Tanujjal Bora
	Dr. Dieter Wilhelm Trau
Nationality:	Thai
Previous Degree:	Bachelor of Engineering in Biomedical Engineering
	King Mongkut's University of technology North Bangkok, Bangkok, Thailand
Scholarship Donor:	Royal Thai Government Fellowships

Asian Institute of Technology
School of Engineering and Technology
Thailand
July 2022

AUTHOR'S DECLARATION

I, Wisanu Simalai, declare that the research work carried out for this thesis was in accordance with the regulations of the Asian Institute of Technology. The work presented in it are my own and has been generated by me as the result of my own original research, and if external sources were used, such sources have been cited. It is original and has not been submitted to any other institution to obtain another degree or qualification. This is a true copy of the thesis, including final revisions.

Date: 22 July, 2022

Name (in printed letters): Wisanu Simalai

Signature: 

ACKNOWLEDGMENTS

With so much difficulty and challenge, I would like to express my deep gratitude to Dr. Ricco, my advisor, who has always supported and recommended me throughout the research, especially regarding complex processes and solutions from laboratory constraints. Working with him and learning under his direction was a privilege, which helped develop many of the abilities required for chemistry and biology research. I would like to thank my committee, Dr. Tanujjal Bora, for some advice and questions which prompted me to review the results of the research experiments and theories. I am grateful to Apichaya Chantaraklud, PhD student, for her advice and guidance on using laboratory equipment and instruments and recommendations for ZnONR synthesis under optimal conditions. I would like to thank my parents for their financial support, encouragement, and concern for education and work. Finally, I would like to thank my friends and research colleagues for always exchanging knowledge, helping and encouraging me. I hope we will have the opportunity to work together in the future.

ABSTRACT

Infectious diseases are one of the main problems that cause rapid morbidity or mortality, especially with emerging epidemics. The rapid detection of infectious diseases is an essential factor in preventing, diagnosing, and treating transmission. Therefore, the design and fabrication of biosensors for detecting pathogens is one of the critical factors for promptly screening and identifying infected people. Immunosensors are a class of biosensors relying on antibody-antigen interactions, which have an attractive option for developing diagnostic tools such as home use and Point-of-Care (POC). Metal-organic frameworks (MOFs), thanks to their large surface area, high porosity, structural diversity, and tunable composition, metal-organic frameworks (MOFs) can help improve antibody immobilization efficiency to increase stability and controllable orientation. In particular, a subset represented by zeolitic imidazolate framework-C (ZIF-C), consisting of Zn^{2+} and 2-methylimidazole, can be produced around the Fc region of the antibody since Zn^{2+} accumulates on the negatively Fc region. Therefore, the Fc regions are partially embedded within the MOF, and the antibody-binding areas protrude toward the exterior part of the material. In this study, a model immunosensor based on an anti-albumin antibody will be optimized by using selective growth of oriented Abs into the ZIF-C nanocrystals on ZnO nanorods substrate (ZnO@ZIF-C*Ab). The efficiency, surface structures, and chemical elements of the immunosensor will be evaluated by Scanning Electron Microscopy (SEM), Energy Dispersion X-ray Spectroscopy (EDX), UV-VIS absorption spectroscopy, and Fluorescence spectroscopy on the FITC-tagged albumin.

Keywords: Infectious disease, biosensor, immunosensor, immobilization, Metal-organic framework, zeolitic imidazolate framework-C

CONTENTS

	Page
ACKNOWLEDGMENTS	**iii**
ABSTRACT	**iv**
LIST OF TABLES	**vii**
LIST OF FIGURES	**viii**
LIST OF ABBREVIATIONS	**x**
CHAPTER 1 INTRODUCTION	**1**
1.1 Background of the Study	1
1.2 Statement of the Problem	4
1.3 Objectives of the Study	7
1.4 Scope of the Study	7
1.5 Limitations of the Study	8
1.6 Organization of the Study	8
CHAPTER 2 LITERATURE REVIEW	**9**
2.1 Detection Techniques for Infectious Diseases	9
2.1.1 Molecular Assays	9
2.1.2 Immunological Assay	10
2.2 Antibody-based Immunosensors	12
2.2.1 Antibody Structure	13
2.3 Methods for the Immobilization of Antibodies on Various Surfaces	13
2.3.1 Non-Covalent Immobilization	14
2.3.2 Trapping Technique Immobilization	14
2.3.3 Covalent Immobilization	15
2.3.4 Affinity-based Immobilization	15
2.4 Porous Materials as Novel Tools for the Immobilization of Biomolecules of Interest	16
2.4.1 Bio-composite Immobilization and Protection with MOFs Materials	17
2.4.2 Antibody Immobilization with Zeolitic Imidazolate Frameworks-8 (ZIF-8)	19
2.5 Chapter Summary	22

		Page
CHAPTER 3 METHODOLOGY		**24**
3.1	Research Diagram	24
3.2	Surface Modification of Glass Substrates	25
3.2.1	Synthesis of Zinc Oxide Nanorods (ZnONRs) on Glass Substrates	25
3.2.2	Conversion of ZnO into ZIF-C Framework (Control Experiment)	26
3.2.3	Conversion of ZnO into ZIF-C*Ab Framework (Sample Fabrication)	26
3.3	Immunosensor Performance Evaluation	27
3.3.1	Preparation of Fluorescein-Human Serum Albumin Solution	27
3.3.2	Sensitivity Detection Testing of the Fluorescence-based Immunosensor	27
3.3.3	Selectivity Detection Testing of the Fluorescence-based Immunosensor	28
3.4	Characterization of the Immunosensor	29
CHAPTER 4 RESULTS AND DISCUSSION		**30**
4.1	Characterization and Morphology of ZnONR Substrates	30
4.1.1	Characterization of the ZnONR Structure	30
4.1.2	UV-Visible Spectroscopy Characterization of the ZnONR	31
4.2	Characterization of ZnONR to ZIF-C Conversion	32
4.2.1	Transformation of ZnONR to ZIF-C Structure	32
4.2.2	Optimization of Variables: Time, Concentration, Buffer Composition	33
4.3	Conversion of ZnONR to ZIF-C*Ab	36
4.4	The Detection of Human Serum Albumin (HSA) and Evaluation of Antibody Immobilization	38
4.4.1	Testing of Specific and Non-specific Binding	39
4.4.2	Sensitivity of HSA Detection	39
CHAPTER 5 CONCLUSION AND RECOMMENDATIONS		**42**
5.1	Conclusion	42
5.2	Recommendation	42
REFERENCES		**44**

LIST OF TABLES

Tables	**Page**
Table 1.1 The Epidemics Caused by a Virus	2
Table 2.1 The Different Immobilization Approaches with MOFs	18
Table 3.1 The List of Characterization Techniques	29

LIST OF FIGURES

Figures		Page
Figure 1.1	The Diagram of the Biosensor System	4
Figure 1.2	Metal-Organic Framework Structure	6
Figure 2.1	The Structure of Antibody	13
Figure 2.2	The Different Immobilization Techniques on Biosensor Substrate	14
Figure 2.3	a) Schematic diagram of ZnO@ZIF-8 PEC Sensors with Selectivity to H_2O_2. b) Photocurrent Response of the Sensor in the Presence of H_2O_2 (0.1 mM) and Ascorbic Acid (0.1 mM)	17
Figure 2.4	a) ZIF-8 Structure from Zn^{2+} and 2-methylimidazole. b) the 145˚ Angle of Methylimidazole (HmIm) Ligand between Zinc and HmIm.	19
Figure 2.5	The Preparation Diagram of ZnO@ZIF-8/Ionic Liquid/Myoglobin-Chlorinated Polyethylene and Zno@ZIF-8/Ionic Liquid/ Glutaraldehyde/Anti-IgG/BSA/IgG-Chlorinated Polyethylene	20
Figure 2.6	The ZIF-8 Coating on Fe_3O_4 Particles for Antibody Fragments Immobilization	21
Figure 2.7	The Antibody Protection Testing by Using ZIF-8 Coating	21
Figure 2.8	The Schematic of the ZIF-C*Ab Crystallization Process	22
Figure 3.1	Diagram of Zno Nanorods Synthesis	25
Figure 3.2	The Conversion of ZnO into ZIF-C Framework of ZnO Nanorods Substrate	26
Figure 3.3	The Conversion of ZnO into ZIF-C*Ab on the Substrate	27
Figure 3.4	The Sensitive Immunosensing Evaluation with Fluorescence Spectroscopy	28
Figure 3.5	The Selective Immunosensing Evaluation	28
Figure 4.1	The Diameter Comparison of the a)5 mM, b)10 mM, c)15 mM, and d)30 mM of ZnONR Concentrations in SEM Characterization; e) Correlation Graph Between Concentration and ZnONR Diameter	30
Figure 4.2	The Morphology of ZnONR in a) the Top View and b) Diameter Histogram, and c) Cross-section View	31
Figure 4.3	UV-Visible Spectrum of ZnONR	31

Page

Figure 4.4 The SEM Characterization of ZIF-C Structures on ZnONR in the a) Top-view and b) Cross-section 32
Figure 4.5 a) The UV-Visible Absorbance Spectrum in Different Layers and b) Water Contact Angle Measurement of ZnONR and ZIF-C 33
Figure 4.6 The Water Contact Angle Measurement of ZIF-C, Synthesized with Different HmIm Concentrations 34
Figure 4.7 The Time Conversion of ZIF-C on ZnONR Surface Monitored via WCA 35
Figure 4.8 The ZIF-C Conversion Approach in Different Buffers (Pretreatment/Washing) 36
Figure 4.9 The Water Contact Angle Measurement of Different Sample Layers 37
Figure 4.10 The FTIR Spectra of ZIF-C, ZIF-C*Ab, and ZIF-C*Ab/HSA 38
Figure 4.11 The Fluorescence Spectra of before and after HSA-FL Mixing 39
Figure 4.12 The Evaluation of Specific and Non-specific Binding to HSA 40
Figure 4.13 The Relationship between HSA-FL Concentration and Fluorescence Intensity 41
Figure 4.14 The Immunosensor Sensitivity of HSA Detection 41

LIST OF ABBREVIATIONS

Ab	Anti-Human Serum Albumin monoclonal antibody
CDC	Centers for Disease Control and Prevention
COVID-19	Coronavirus disease 2019
DMF	N,N-dimethylformamide
DNA	Deoxyribonucleic acid
FL	Fluorescein
Flu	Influenza
HmIm	2-methylimidazole
HSA	Human Serum Albumin
IMS	Immunomagnetic separation
LAMP-PCR	Loop-mediated isothermal amplification
LoD	Limit of Detection
MOF	Metal-Organic Framework
MOPS	(3-(N-morpholino)propanesulfonic acid)
POC	Point-of-Care
PCR	Polymerase Chain Reaction
RT-PCR	Reverse Transcription-Polymerase Chain Reaction
RNA	Ribonucleic acid
SARS	Severe Acute Respiratory Syndrome
SPR	Surface Plasmon Resonance
WCA	Water Contact Angle
WHO	World Health Organization
ZIF	Zeolitic Imidazolate Frameworks

CHAPTER 1
INTRODUCTION

1.1 Background of the Study

Infectious diseases can cause rapid mortality, especially with emerging epidemics towards which remedies are not efficient. Infectious diseases pose a significant threat to human life. They are brought by several pathogens like bacteria, fungi, viruses, or helminths, and can be transmitted through contact with infected people, animals (e.g., zoonosis), or contaminated objects. The term “infectious diseases” refers to any disease transmitted from one person or animal to another (Kotra, 2007). Symptoms depend on the type of disease and vary in severity. However, the most common symptoms of infectious disease are fever, diarrhea, fatigue, muscle aches, and cough (Kotra, 2007).

There has been a sharp rise in emerging infectious diseases observed in recent years or recognized as a threat to public health. The emergence of these new diseases is a stark reminder that the health of populations worldwide is still at risk. The World Health Organization (WHO) defines an emerging infection as a disease that has recently emerged or re-emerged in each region or setting previously not detected (World Health Organization, 2015). Emerging infections can be caused by old and new pathogens, including unclassified organisms with the following diseases in **Table 1.1**.

The rapid development of tourism and the economy has resulted in increased international travel, with consequent diffusion of diseases worldwide. As a result, several countries experience regular or extraordinary epidemics of respiratory conditions such as Influenza, Avian influenza, Zika Virus, Severe Acute Respiratory Syndrome (SARS), and, most recently, Coronavirus disease 2019 (COVID-19) (Li et al., 2020). To reduce the impact of epidemics, the quick detection of infectious diseases is one of the essential factors in preventing, diagnosing, and treating transmission.

Table 1.1

The Epidemics Caused by a Virus

Disease	Cause and Common symptoms	Outbreaks	References
Coronavirus Disease	Cause - By SARS-CoV, MERS-CoV, SARS-CoV-2 - Transmission from person to person by respiratory droplets Symptoms - Fever - Dry cough - Dyspnea - Diarrhea - Sore throat	MERS: 2012, 2015, 2018 SARS: 2002-2004 COVID-19 : 2019-current	(National Foundation for Infectious Diseases, 2021)
Influenza	Cause - By influenza virus has 4 types (A virus, B virus, C virus, and D virus) - Transmission in coughing or sneezing fluid and by touching contaminated surfaces Symptoms - Fever - Chills - Aches - Cough - Sore throat	Occurred in 1900 Spanish flu: 1918-1920 Asian flu: 1957 Hong Kong flu: 1968 Russian flu: 1977 Swine flu: 2009	(Centers for Disease Control and Prevention, 2020). (Kalil & Thomas, 2019).
Adenovirus-es	Cause - By Adenoviruses - Transmission from touching a person or an object, sometimes from infected stool Symptoms - Fever - Bronchitis - Sore throat - Pneumonia - Gastroenteritis	In France: 1956 In the USA: 1973 In England: 1974 In Sweden: 1976-1977	(James et al., 2007) (Biggs et al., 2018) (Wadell et al., 1980)

To cope with such pandemics, laboratory detection of infectious diseases may not be sufficiently fast when conducted on a large scale, due to the rapidly spread of the infection occurring in a short period. Therefore, many diagnostic equipment manufacturers seek to develop modern, rapid, highly accurate, and cost-effective detection devices, also usable in non-laboratory settings (Anna MacDonald, 2020; Cai et al., 2020). Therefore, the design and fabrication of biosensors for detecting pathogens is a challenge for manufacturers and is one of the critical factors for promptly screening and identifying infected people.

Immunosensors are a class of biosensors relying on antibody-antigen interactions. The Antibody (Ab) is immobilized on the substrate and acts as the biological recognition element towards the antigen (Ag) analyte. The design of immunosensors for detecting specific diseases is essential to medical diagnostics in preventing the spread of infections. Immunosensors normally consist of (biological) receptors / transducers / processors. As shown in **Figure 1.1**, receptors detect specific target molecules, producing change, such as thermal, electrical, and fluorescence, which is converted into electrical signals with a transducer; the signal is then analyzed by the processor (Needs, 2018; Zea et al., 2020).

The specificity of the antigen-antibody interaction is an attractive option for developing diagnostic tools suitable for home use and Point-of-Care (POC) (Cristea et al., 2015). For example, the detection of Legionella pathogenic bacteria has been reported with electrochemical immunosensors using ZnO nanorods (Park et al., 2014). The nanorods were prepared by a low-temperature hydrothermal method for antibody immobilization with electrostatic reaction. When the antigen is detected in an ELISA-like test, it is possible to quantify it in the range of 1-5000 pg/mL, with a limit of detection (LOD) of 1 pg/mL.

Figure 1.1

The Diagram of the Biosensor System

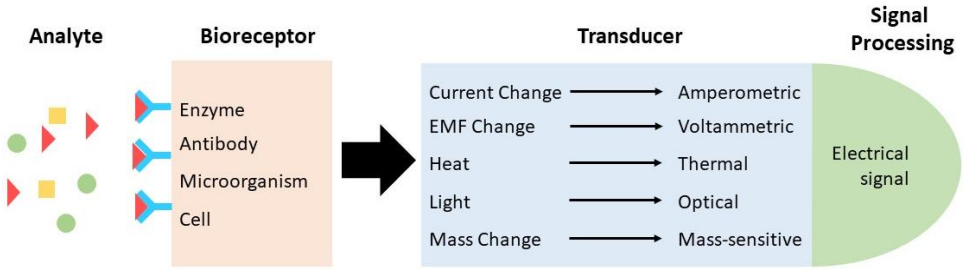

There are many developments in immunosensors to meet the demands of clinical and industrial applications. The novel design using nanoparticles and nanostructured surfaces improved antibody immobilization efficiency and a better ability to bind target molecules. Therefore, using immunosensors leads to faster clinical decision-making, lower cost of examinations, and reduced workload for healthcare professionals (Cristea et al., 2015).

1.2 Statement of the Problem

Biosensors are now widely used in industrial, medical, environmental, military, and many other fields, classified according to the type of biological receptors and transducers. For immunosensors aimed at recognizing antibodies, the design of the substrate needs to be consistent with the sensor type, such as the properties of surface plasmon resonance (SPR) of gold nanoparticles (Wijaya et al., 2011). However, the sensor's surface designed for detection needs to be modified to immobilize antibodies on the substrate, for example, by increasing the surface area with porous material, coating with an adhesion-enhancing material, or using covalent bonding (Reimhult & Höök, 2015).

Antibody immobilization on the sensor surface is essential in developing immunological assays to reduce detection steps and time. In addition, the substrate should have physical and chemical stability and a high-affinity functional group. The chemistry of immobilization should be cost-effective, easy to use, and prevent the leaching of immobilized antibodies, including controlling their orientation (Vashist & Luong, 2018). Currently, there are several techniques for immobilizing Abs with different advantages and disadvantages, especially the correct direction of the immobilized Abs (Brückner et al., 2021).

Physical adsorption is a traditional method for direct Ab immobilization, which is easy to use and cost-effective, but it has drawbacks in terms of stability, low reproducibility, and uncontrollable orientation (Ruiz et al., 2019; Taheri et al., 2016). On the other hand, although covalent conjugation increases the likelihood of more efficient Ab immobilization due to irreversible binding on the substrate surface, difficulties remain with the proper orientation (Lou et al., 2018). Furthermore, since the immobilized Ab conjugate position has a significant effect on the possibility of specifically targeting the molecule, the crystal fragment (Fc) is usually the optimal anchoring location, as the antigen-binding fragment (Fab) will protrude outside of the surface (Gao et al., 2021).

Recently, a new Ab immobilization technique has been developed exploiting the strong affinity between sulfhydryl groups and gold nanoparticles, allowing them to be readily adsorbed on single-chain variable fragments of the antibody and immobilized on Au substrate. However, due to this covalent bond, the orientation of the antibody is "Side-On," where the antibody lies down sideways, resulting in a decreased ability to bind the antigen (Welch et al., 2017). Alternatively, covalent immobilization of IgG-binding protein A or G is useful for orientation control due to its ability to adsorb the Fc region of the antibody selectively. Additionally, the conjugation between A/G and IgG proteins cannot be dissociated unless highly high temperature and organic solvent are used (Ingavle et al., 2015).

To improve the antibody immobilization efficiency to high stability and controllable orientation, novel biocomposites based on porous materials are exciting areas for research and development (Doonan et al., 2017; Velásquez-Hernández et al., 2021). Furthermore, combining organic and inorganic biocomposites can lead to improved or novel properties. The result is a bio-composite especially interesting for biotechnology and biomedical applications (McKinlay et al., 2010).

Metal-organic frameworks (MOFs) are porous materials made of metal centers interconnected with organic molecules ligands, as shown in **Figure 1.2**. Due to their large surface area, high porosity, structural diversity, and tunable composition, MOFs are used as novel materials in a wide variety of applications such as carbon captures, biomedical microrobots, chemical separation, catalysis, sensing applications, encapsulation and site-specific conjugation (Paolo Falcaro et al., 2016; Feng et al., 2019; Ricco et al., 2016). In addition, the structure of the MOF can be modified and

controlled at the molecular level, allowing the porosity and surface to be changed after synthesis (Furukawa et al., 2013; Z. Wang & Cohen, 2009). For example, wide porosity and high surface area MOFs control the absorption or release of large molecules (Rojas et al., 2019), whereas narrow pore MOFs are used in analytical detection and selection applications (Huo et al., 2015).

Figure 1.2

Metal-Organic Framework Structure

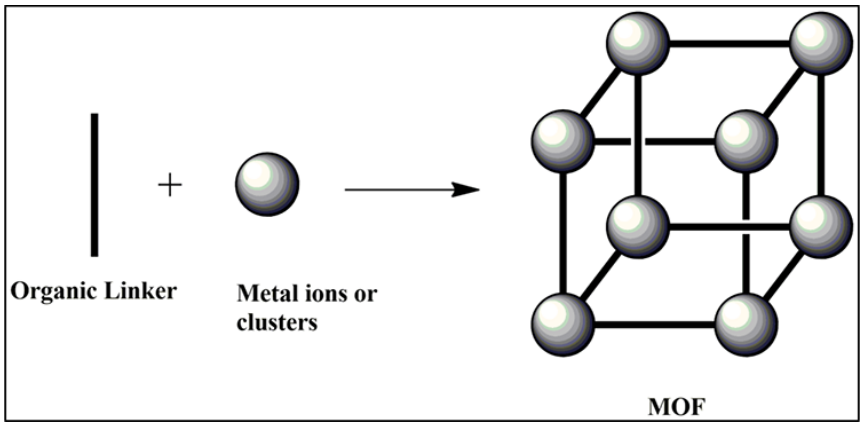

Note. Adapted from (Sharmin & Zafar, 2016)

To achieve biocomposites that correspond to applications, there are various strategies for integrating biomolecules into MOF like encapsulation, bioconjugation, and infiltration. The use of MOFs for encapsulating biological organisms such as proteins, cells, vaccines, etc., is to protect them when subjected to unacceptable environmental conditions that can compromise their functional potential during transport and storage (K. Liang, Ricco, et al., 2015). For example, Antibodies were encapsulated within zeolitic imidazolate frameworks (ZIFs) to protect them from temperature and solvents (C. Wang et al., 2018). For bioconjugation, biomolecules are immobilized on the MOF surface by covalent bonds or physical adsorption, whereas for infiltration, biomolecules are immobilized within the MOF pore network via a diffusion process.

Recently, Qi et al. presented a strategy for controllable antibody immobilization on the surface of MOFs (Qi et al., 2017). Antibodies were biotinylated on the COOH-rich MOF surface to improve bio-detection. Maddigan et al. demonstrated that ZIF-8 consists of Zn2+ and 2-methylimidazole spontaneously self-assembles on proteins with isoelectric points lower than 7 (Maddigan et al., 2018). Zn2+ concentrates on negatively

charged functional groups on the surface of biomacromolecules, allowing ZIF-8 to form rapidly; conversely, in the presence of positively charged proteins, ZIF-8 self-assembly did not occur (Maddigan et al., 2018; Qi et al., 2017).

As anticipated, the antibody's structure is divided into the Fab and Fc regions, with significantly different charge distributions between both areas (W. Zhang et al., 2020). The Fab region of an antibody contains positively charged amino-terminal groups, whereas the Fc region contains negatively charged carboxyl and histidine groups. Therefore, the immobilization of antibodies onto the MOF is expected to induce the spatial-controlled crystallization of Zn-based ZIF primarily around the Fc region, and thereby the orientation-controlled antibody can be easily performed by immobilization on this kind of MOF (see Chapter 2 for a detailed discussion of this specific case).

1.3 Objectives of the Study

This study aims to design and develop antibody immobilization on the substrate of a fluorescence-based immunosensor for the detection of infectious diseases, improving the efficiency of surface immobilization of antibodies used in fluorescence-based immunosensors to detect infectious diseases, such as SARS-CoV-2. For this purpose, the substrate surface will be modified with Zinc Oxide nanorods, which will then be converted into a ZIF-based material (Alt et al., 2021; P. Falcaro et al., 2020; Velásquez-Hernández et al., 2021). The specific objectives of the research are as follows:

1. Surface modification of glass substrates for the direct immobilization of antibodies.
2. Fabrication of surface-bound antibodies on the prepared substrates, via the conversion of a ZnO-based support adsorbing Abs into a Metal-Organic Framework (MOF) called ZIF-C (Falcaro et al., 2020; M. de J. Velásquez-Hernández et al., 2021).
3. Evaluation of the performance of the immunosensor towards a model protein, acting as a testbed for SARS-CoV-2, and estimation of parameters like limit of detection, sensitivity, and selectivity.

1.4 Scope of the Study

The scope of this research is in the field of nanotechnology and biosensors, which deals with the design and evaluation of antibody immobilization on the surface of sensors focused on the detection of epidemic respiratory infections, such as influenza, SARS,

and COVID-19. For the design of immunosensors, a Metal-Organic Framework (MOF) is prepared onto the substrate to favor the orientation-controlled antibody immobilization. The efficiency of the immunosensor will be tested with the help of different techniques, such as UV-VIS spectroscopy, fluorescence spectroscopy, scanning electron microscopy (SEM), and others.

This process aims to simplify the surface immobilization of antibodies by directly anchoring them on a porous material that self-assembly in the presence of both the ligand and the metal source. Furthermore, the use of ZnO already grown on the substrate allows for a direct immobilization, whereas the ability to grow this ZnO on almost any kind of substrate (glass, plastic, paper, etc.) improves the versatility of the process, at the same time eliminating the need of covalent bonding and the utilization of complex functional groups and chemical reaction. Finally, since the reaction of conversion/immobilization occurs in water at room temperature for a few minutes, the process is mild, fast, economically viable, and environmentally friendly.

1.5 Limitations of the Study

- Human Serum Albumin (HSA) is used to evaluate antibody immobilization instead of pathogenic antigens or proteins due to laboratory limitations and safety.
- Antibody Immobilization was only performed on the glass slide substrate with the ZIF-C self-assembly technique.
- The storage time and conditions of the biosensor are not evaluated.
- The test and evaluation of the detection of immunosensors is a laboratory study, not used commercially.

1.6 Organization of the Study

This thesis is organized in the following structure:

Chapter 1: Introduction

Chapter 2: Literature Review

Chapter 3: Methodology

Chapter 4: Results and Discussion

Chapter 5: Conclusion and Recommendations

CHAPTER 2
LITERATURE REVIEW

Currently, the public health and medical systems have greatly advanced in dealing with infectious diseases, also severe and mutated ones. However, making accurate and quick diagnoses is essential to treating and preventing the spread, requires modern technologies, which are portable, cheap, user-friendly, and accurate, to be widely used in clinical applications for detection.

2.1 Detection Techniques for Infectious Diseases

Diagnosis and detection of infectious diseases are critical for disease identification, treatment, and prevention. The physician first determines the symptoms and risk factors if a patient is suspected of having an infection. Individual symptoms vary according to the type of pathogenic microorganism, which may be bacteria, viruses, fungi, or parasites. Therefore, tests to confirm infection can be determined by the pathogen's antigen, antibody, or nucleic acid.

2.1.1 Molecular Assays

The molecular assay detects nucleic acids in microorganisms whose nucleic acids consist of deoxyribonucleic acid (DNA) or ribonucleic acid (RNA). The starting point for molecular techniques is the inability of some pathogens to be cultured and traditional diagnostics involve complex methods and long incubation times (Vouga & Greub, 2016; Yang & Rothman, 2004). Therefore, amplified nucleic acids are effective in clinical medicine for detecting pathogens such as viruses, bacteria, and parasites (Zauli, 2019). Currently, there are a variety of nucleic acid amplification techniques such as Polymerase Chain Reaction (PCR), LAMP-PCR, digital PCR (dPCR), real-time PCR (qPCR), and Reverse transcription-polymerase Chain Reaction (RT-PCR).

2.1.1.1 **Polymerase Chain Reaction (PCR)** PCR is a technique for amplifying DNA fragments in the laboratory, in which the number of molecules increases exponentially with each reaction step, making it easier to diagnose an infection (MENON et al., 1999). It is commonly used to quantify and detect bacteria and viruses in infected specimens such as urine, blood, saliva, and sweat. Because of the sensitivity, specificity, and rapidity of PCR, this diagnostic technique has an incredible ability to identify very small amount of genetic fragments, thus being suitable to organisms that

are poorly able to be cultured or require long incubation periods (Louie et al., 2000). For example, early detection of Tuberculosis, which causes respiratory disease, is essential for diagnosis and effective treatment. PCR has a much greater potential than traditional culture techniques in disease identification (Singh & Kashyap, 2012). PCR has also been developed into other speciality techniques as follows.

2.1.1.2 **Loop-Mediated Isothermal Amplification (LAMP-PCR)** LAMP-PCR is a new molecular diagnostic technique that can detect multiple pathogens simultaneously. The method relies on DNA polymerase and a unique set of primers recognising different target DNA sequences (Iwamoto et al., 2003). Furthermore, unlike thermocycler-based PCR, the amplification phase requires only a single temperature stage for the reaction. LAMP-PCR is not only suitable for detecting and identifying bacteria but is also developed to detect parasites and viruses (Varlet-Marie et al., 2018). In 2017, Kurosaki et al. developed the LAMP-PCR assay to detect the Zika virus (ZIKV) from plasma, serum, and urine (Kurosaki et al., 2017).

2.1.1.3 **Real-time PCR (qPCR)** Real-time PCR, based on quantitative PCR (qPCR), is a technique developed for detecting and quantifying pathogens using fluorescent reagents. In qPCR, the target molecule is detected in real-time and does not require post-processing, thus reducing the risk of causing a false-positive result (Sibley et al., 2012). In addition, the qPCR technique is susceptible and specific compared to serological tests, especially in diagnosing epidemics. For example, it has been used to detect ZIKV in human urine, as it has a residence time of up to 20 days, suggesting that it is easier to see in such biological fluid rather than serum tests (Wahid et al., 2016).

2.1.1.4 **Reverse Transcription-Polymerase Chain Reaction (RT-PCR)** RT-PCR is a standard technique for RNA virus identification by amplification of viral genetic material in a sample. This technique requires the conversion of viral genomic RNA into a short complementary DNA copy (cDNA) and its subsequent amplification by PCR (VanGuilder et al., 2018). Given the COVID-19 outbreak, RT-PCR testing is essential for the rapid and accurate diagnosis of infection using samples from the upper respiratory tract, including saliva and ocular secretions (Xia et al., 2020).

2.1.2 Immunological Assay

An immunoassay is a biochemical test based on detecting antigens or antibodies of target molecules in samples from an infected person, such as serum, urine, and blood (Yetisen et al., 2013). Typically, the analyte is bound as an antigen or protein to an antibody peculiar to the target molecule, forming an antigen-antibody complex. On the

other hand, an immunoassay may use antigens to detect antibodies, known as an antibody test. After binding the antigen to the antibody in the immunoassay, the measurable signal manifests itself in various forms such as radiation emission, color change in solution, and fluorescence (Peruski et al., 2003). Various biochemical detection methods are available today, such as enzyme-linked immunoassay, lateral flow assay, and magnetic separation.

2.1.2.1 **Enzyme-Linked Immunosorbent Assays (ELISA)** ELISA is a solid-phase test using enzyme-linked reagents that are sensitive to the detection of antigens and antibodies. The principle of this technique is chemically coupled labeling of enzymes when the antigen-antibody bond forms a solid phase complex (Engvall & Perlmann, 1971). The result is a color yield directly visible and quantitatively measured by absorption or fluorescence intensity. The advantages of this technique are economical, versatile, robust, and simple assays that make ELISA a reliable screen for small sample volumes and can be used in various applications such as epidemiology and diagnostics (Katti, 2001). For example, detecting and quantifying SARS-CoV-2 in blood, plasma, or serum samples, may be either qualitative or quantitative and used in laboratories (West & Kobokovich, 2020). This test takes approximately 1-5 hours for COVID-19, where antibodies bind to viral proteins and can detect antibody-protein complexes by color or fluorescent readings (Carter et al., 2020).

2.1.2.2 **Immunochromatographic Lateral Flow Assays (LFA)** This test is used in infectious disease detection, drug quantification in biological fluids, and food safety testing (Zuk et al., 1985). The test is easy to use and takes as little as 15 minutes by dropping the test sample onto the test strip, after which a binding of the sample's antigen and the labeled and fixed antibody is established on the strip (Beck et al., 2000). However, there are several limitations: the detection of only one substance per test strip, the analytical sensitivity varies with substantial weight, and the qualitative test (Ortega-Vinuesa & Bastos-González, 2001).

2.1.2.3 **Immunomagnetic Separation (IMS)** IMS is used to efficiently separate particles and antigens from liquids and detect pathogens (Ugelstad et al., 1993). In principle, IMS separation involves capturing molecules by attaching small magnetic particles or beads that are gradually separated by multiple wash cycles to obtain the target molecule (C. Sun et al., 2017). These beads contain paramagnetic magnets (Fe_3O_4), which give this technique the advantage of rapidly separating the antibody-

binding material from the environment when placed in a magnetic field (Haukanes & Kvam, 1993; Lisi et al., 2012).

2.2 Antibody-based Immunosensors

Immunosensors are solid-state devices that recognize an antigen-specific molecule by antibodies immobilized on the substrate and coupled to a transducer. The minor difference between immunosensor and immunoassay is that the immunoassay depends on the recognition process of the antigen, which takes place elsewhere, whereas the immunosensor has an immunocomplex formation and analysis on the same platform (Hosu et al., 2018; Y. Wang et al., 2008; Warsinke et al., 2000). However, due to the high sensitivity and selectivity of immunochemical, immunosensors are valuable tools in various applications, including clinical diagnostics and research, making analysis much easier, faster, and more reliable (S. L. Liang & Chan, 2007).

Immunosensors can be classified according to the types of transducers, such as electrochemical (amperometric, potentiometric, conductometric, and impedance), optical (refractive index, fluorescence, luminescence), and piezoelectric (Mistry et al., 2014). These sensors can be either direct (label-free) or indirect (labeled) immunosensor. Label-free immunosensors can directly measure the presence of the analyte via the physical or chemical changes on a transducer surface. These sensors can be used for real-time analysis and therefore have more clinical applications. However, they are significantly affected by the nonspecific adsorption reaction, which causes a small interference magnitude due to the nonspecific binding of antigens or other proteins on the substrate surface (Daniels & Pourmand, 2007; Jiang et al., 2008; Rapp et al., 2010; Vestergaard et al., 2007).

On the other hand, labeled immunosensors rely on signal generation by unique labels that may contain one or more markers. Tags used in immunosensors include enzymes, gold nanoparticles (AuNPs), quantum dots (QDs), fluorophores, and radioisotopes. The advantages of labeled immunosensors are higher sensitivity and less impact of nonspecific adsorption on the signal. However, the efficacy of antigen-binding antibodies may be reduced due to variability in labeling responses (Oswald et al., 2000). Immunosensors have become particularly important for point-of-care and home applications due to their low cost and small size. Immobilization techniques and

biological components such as antibodies, aptamers, and RNA are important for developing sensor designs (Cristea et al., 2015).

2.2.1 Antibody Structure

Antibodies are a type of glycoprotein that plays a crucial role in immune system defense mechanisms and are produced by B lymphocytes. Antibodies are divided into five classes: IgM, IgD, IgG, IgE, and IgA, which are Y-shaped, and their basic structure is divided into the fragment antigen-binding (Fab) region and the fragment crystallizable (Fc) region, as shown in figure 2.1 (AVRAMEAS et al., 1978; BioExplorer.net, 2019). The antibody (Ab) has four polypeptide chains consisting of two identical light chains and two heavy chains linked by disulfide bonds. The key Fab site that makes the antibody highly specific for the antigen (Ag) is the complementarity determining region (CDR) (Conroy et al., 2009). Thus, the Ag-specific Ab site is the paratope, and the augmented area on Ag-specific Ab is its epitope.

Figure 2.1

The Structure of Antibody

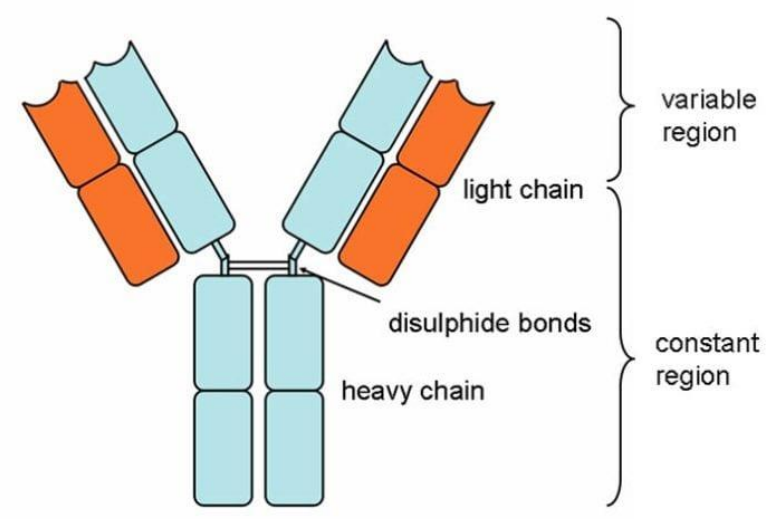

2.3 Methods for the Immobilization of Antibodies on Various Surfaces

In addition to biological composition, the technique for immobilizing antibodies on the substrate surface also plays a vital role in developing and improving higher efficiency. Appropriate immobilization methods allow for the stable biological activity of the antibody and good orientation where binding sites to the analyte are exposed (Luppa et al., 2001). Moreover, antibody immobilization must not alter the specificity and biological activity. Therefore, the immobilization procedure affects the efficiency,

specificity, sensitivity, and limit of detection (LoD) of the immunosensor with several techniques, as shown in **Figure 2.2** (Trilling et al., 2013).

Figure 2.2

The Different Immobilization Techniques on Biosensor Substrate

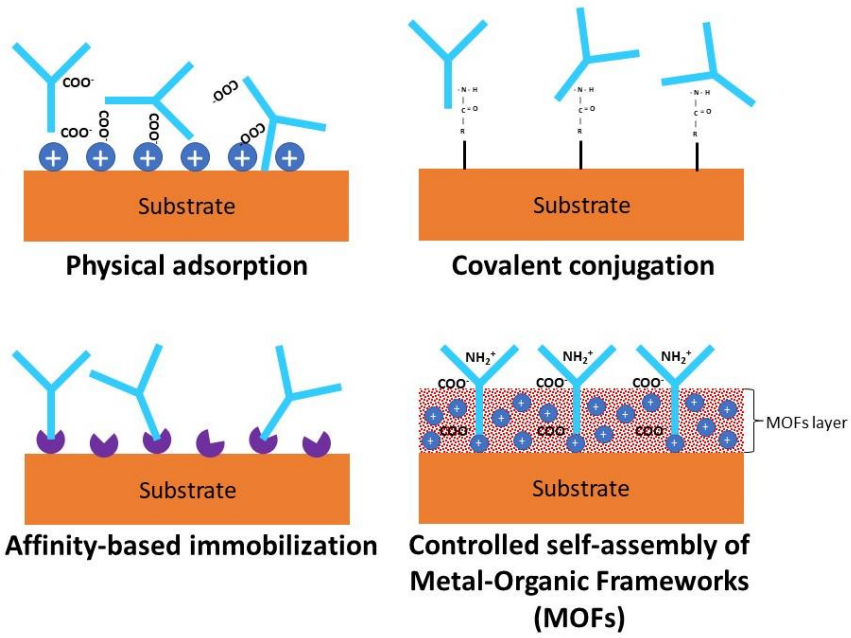

2.3.1 Non-Covalent Immobilization

The non-covalent immobilization technique, such as physical adsorption and chemical adsorption, is a method that uses electrostatic force, hydrophobic reaction, and Van der Waals force. Although physical adsorption is a simple method to bind antibodies to the substrate, it has some limitations when the concentration of the immobilized antibody has a very low compaction density. In addition, some factors may worsen immunosensor recognition, such as substrate surface contamination, antigen-binding site blockage, and partial denaturation of the antibody (Schramm et al., 1993). Therefore, this technique requires modification of the substrate surface to achieve better absorptivity. For example, a poly-2-cyano-ethylpyrrole coating on gold electrodes increases antibody adsorption and controls proper orientation (Um et al., 2011).

2.3.2 Trapping Technique Immobilization

This method encapsulates biological components that are more stable than physical adsorbents, such as molecularly imprinted polymers (MIPs) and sol-gels (Mollarasouli et al., 2019). In addition, the immobilization method with sol-gel has a simple, low

temperature, biocompatible microenvironment, and low chemical reactivity due to the silica sol-gel network (Luckarift et al., 2004). However, the sensitivity of the immunosensor may be reduced due to the implantation of the antigen-binding site. For example, the silica sol-gel technique has been reported to immobilize anti-carbofuran monoclonal antibodies on the surface of glassy carbon electrodes with a LoD of 0.33 ng/mL (X. Sun et al., 2011).

2.3.3 Covalent Immobilization

Covalent immobilization is the most common method for binding biological components to the substrate surface. Covalent binding requires surface modifications in some substrates or thin-film coatings to provide functional groups for covalent bonding to amino groups of antibodies. Such functional groups are hydroxyl, thiol, carboxyl, or amino (Mollarasouli et al., 2019). Some reagents, such as glutaraldehyde, N-ethyl-N-(3-dimethylaminopropyl) carbodiimide (EDC), and N-hydroxysuccinimide (NHS), are used to make antibodies bind to functional groups on substrates (Sharma et al., 2016).

Alternatively, the self-assembled monolayer (SAM) technique is a semi-covalent binding between the disulfide group and the metal surface, for example, the binding of the antibody to the Au surface by the thiol group (Subbiah et al., 2011; Ulman, 1996). The immobilization with the thiol group has a high affinity and a controllable orientation (Wijaya et al., 2011). In addition, its thin layer formation reduces the analysis time and increases the sensor's sensitivity (Mollarasouli et al., 2019). However, some chemicals can result in the oxidation of amino acids such as methionine, tryptophan, and histidine at the antigen-binding site impairing their binding capacity, with consequent analysis delay due to the loss of biological activity (Shriver-Lake et al., 1997).

2.3.4 Affinity-based Immobilization

The affinity immobilization technique can enhance antibody immobilization and target molecular capture because it has a precisely controlled orientation and reduces partial denaturation (Sharma et al., 2016). This exciting strategy involves binding proteins such as biotin-streptavidin interaction, Protein A or G, Fc-binding peptides, and DNA-directed immobilization (Brena et al., 2013). Streptavidin (or avidin) is widely used to immobilize biomolecules such as proteins, nucleic acids and polysaccharides using biotin-tagged antibodies (Mollarasouli et al., 2019; Sharma et al., 2016). (Strept)avidin-

biotin has the advantages of strong non-covalent interactions, high temperature and pH resistance, and difficulty with protein denaturation (Lesch et al., 2010; Teulon et al., 2011). Immunosensors were developed by Barton et al. using the avidin-biotin interaction, which showed a much higher sensitivity compared to physical-based immobilized immunosensors (Barton et al., 2009). Protein A or G are small bacterial proteins with a high affinity and specificity to the Fc region of the antibody, thus allowing for proper orientation on the substrate (Mollarasouli et al., 2019). An immunosensor developed by de Juan-Franco et al. used a novel, quick, and simple immobilization technique with Protein A-Gold-binding (PAG), which has improved sensitivity and a LoD of 90 ng/ml (De Juan-Franco et al., 2013).

2.4 Porous Materials as Novel Tools for the Immobilization of Biomolecules of Interest

Metal-Organic frameworks (MOFs) are the porous material composed of metal ions acting as templates and organic molecules acting as ligands, which can be one, two, or three-dimensional structures. Due to their large surface area, high porosity, structural diversity, and tunable composition, MOFs are used as novel materials in a wide variety of applications such as carbon captures, biomedical microrobots, chemical separation, catalysis, sensing applications (Falcaro et al., 2016; Otshudiema et al., 2020). For example, sensors for molecular sensing require high selectivity, sensitivity, and analytical velocity, as well as effective electrical, optical, chemical, and physical properties when interacting between analytes and bio-recognition elements on the sensor surface (Kreno et al., 2011; Segev-Bar & Haick, 2013; Wencel et al., 2013).

Today's sensor designs take advantage of MOFs to enhance their performance in selectivity and sensitivity. For example, sensors containing MOFs and metal nanoparticles were reported to be used to monitor the electrochemical dynamics of zinc oxide nanorods, as shown in **Figure 2.3a** (Zhan et al., 2013). For the selectivity of H_2O_2 molecules with ZnO@ZIF-8 nanorods, the ZIF-8 network acts as a filter that allows H_2O_2 or smaller molecules to pass through the ZnO nanorods. In comparison, larger molecules such as ascorbic acid are blocked. The photocurrent test shows the oxidation of H_2O_2 with a wavelength of 380 nm, as shown in **Figure 2.3b**.

Figure 2.3

a) Schematic diagram of ZnO@ZIF-8 PEC Sensors with Selectivity to H_2O_2. b) Photocurrent Response of the Sensor in the Presence of H_2O_2 (0.1 mM) and Ascorbic Acid (0.1 mM)

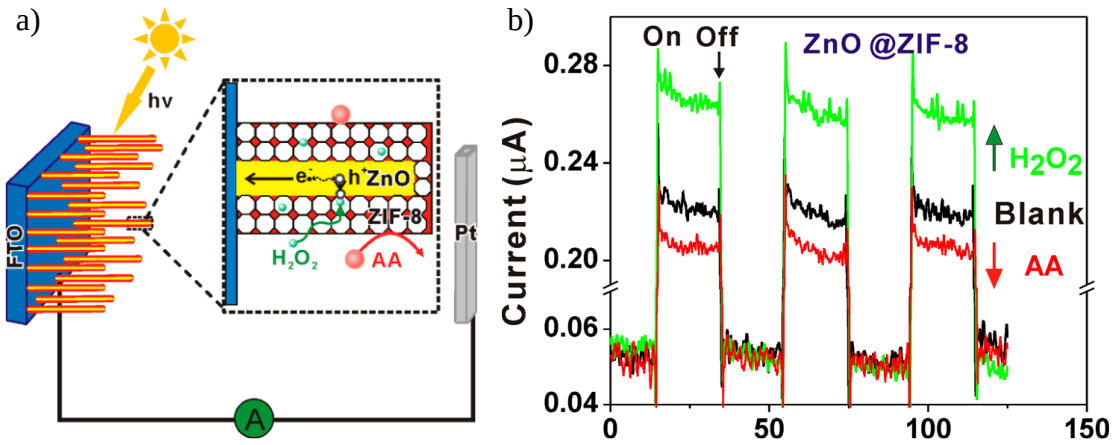

2.4.1 Bio-composite Immobilization and Protection with MOFs Materials

MOFs have the remarkable properties of nanoscale structural design. Based on this advantage, MOFs are utilized to immobilize and encapsulate biological elements such as enzymes, antibodies, and DNA (S. Liang et al., 2020). There are several approaches to combining the composition between MOFs and biomacromolecules by bio-conjugation, infiltration, and encapsulation which have details, advantages, and disadvantages in **Table 2.1** (Doonan et al., 2017).

Table 2.1

The Different Immobilization Approaches with MOFs

Immobilizat-ion Approaches	Definition	Advantages	Drawbacks	References
Surface bioconjugati-on	Physical adsorption: It relies on the electrostatic attraction between the positive charge of the metal in MOFs and the negative charge of the protein. Covalent grafting: MOF ligands have various functional groups, such as carboxylic acids and amino groups, which can serve as anchors for active groups on the surface of biomacromolecules.	simple synthesis process, compatibility with any size biomolecular	weak interaction, easy for leaching, low stability	(Mehta et al., 2016; Pan et al., 2018)
Infiltration into MOFs	The micropores within MOFs allow small molecules to nanoparticles to infiltrate into the MOF. These pores can be designed and controlled to the desired size and structure.	High stability, reduced leaching, high immobilizati-on efficiency	strict particle size requirement for immobilizat-ion, volume, and mass limitations	(Choi & Oh, 2019; Doonan et al., 2017)
Encapsulati-on	Biomolecules are encapsulated within the MOFs. Therefore, particle size can be larger than the micropores of MOFs. MOF crystallinity and immobilization of the biomolecules co-occur in a one-step reaction system.	fewer synthetic steps, high stability, reduced leaching	strictly controlled reaction operation, ratio, and mass limitations of MOFs and biomolecule	(Gkaniatsou et al., 2017; K. Liang, Coghlan, et al., 2015)

2.4.2 Antibody Immobilization with Zeolitic Imidazolate Frameworks-8 (ZIF-8)

Zeolitic imidazolate framework (ZIF) is a subclass of metal-organic framework (MOF) material of interest for scientific and technological research. The structure of ZIF is formed by the interaction between transition metal ions and organic ligands such as Zn^{2+} and imidazole (**Figure 2.4a**). The coordination is by metal and nitrogen atoms at 1,3-position of the imidazole ligand, resulting in a 145 degrees metal-imidazole-metal structure (**Figure 2.4b**) (J. Zhang et al., 2020). As a result, its structure is highly crystalline, has a large specific surface area, and has high stability (Bhattacharjee et al., 2014).

Figure 2.4

a) ZIF-8 Structure from Zn^{2+} and 2-methylimidazole. b) the 145˚ Angle of Methylimidazole (HmIm) Ligand between Zinc and HmIm

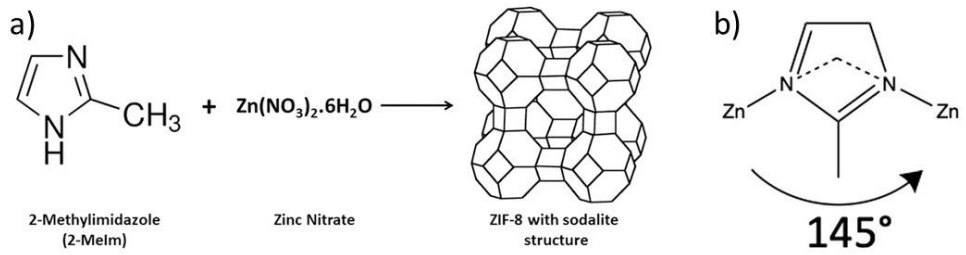

In addition, ZIF-8 has advantages in antibody immobilization on the sensing layer due to flexibility, ultra-high surface area, easy synthesis, and specific binding to the fragment crystallizable (Fc) region of antibodies (Y. Zhang et al., 2020). For example, Wang et al. improved the efficiency of amperometric immunosensors for cancer detection by designing a new probe synthesized using zeolitic imidazolate framework-hydroquinone-bovine serum albumin (ZIF-8-HQ-BSA) (H. Wang & Ma, 2019).

Dong et al. successfully designed an electrochemical immunosensor based on ZnO@ZIF-8, divided into two functions (**Figure 2.5**) (Dong et al., 2017). The first was to study the electrical capability of ZnO@ZIF-8 and myoglobin-containing electrodes with a detection limit of 3.5 µM. Another function was a label-free immunosensor using a ZnO@ZIF-8 composite film as an immobilization substrate. Due to the extraordinary properties of ZnO@ZIF-8, ZnO has good biocompatibility and electrical conductivity, and ZIF-8 has high porosity. Therefore, biosensors based on ZnO@ZIF-8 composite

film have good prospects in developing electrochemical biosensors in terms of good selectivity, repeatability, and stability.

Yim et al. designed a magnetic biosensor to detect pathogenic bacteria in milk. They used ZIF-8 to immobilize half fragments of the antibody via Zn-S bonding, as shown in **Figure 2.6** (Yim et al., 2017). Moreover, ZIF-8 coating on Fe_3O_4 particles can inhibit oxidation. Kang et al. presented a strategy for antibody storage under unrefrigerated with ZIF-8 encapsulation, which enables high-temperature storage, as shown in **Figure 2.7** (Kang et al., 2021). After storage of the ZIF-8-encapsulated antibody, slightly acidic purified water was added and incubated for 1 minute to degrade ZIF-8 for analysis.

Figure 2.5

The Preparation Diagram of ZnO@ZIF-8/Ionic Liquid/Myoglobin-Chlorinated Polyethylene and Zno@ZIF-8/Ionic Liquid/Glutaraldehyde/Anti-IgG/BSA/IgG-Chlorinated Polyethylene

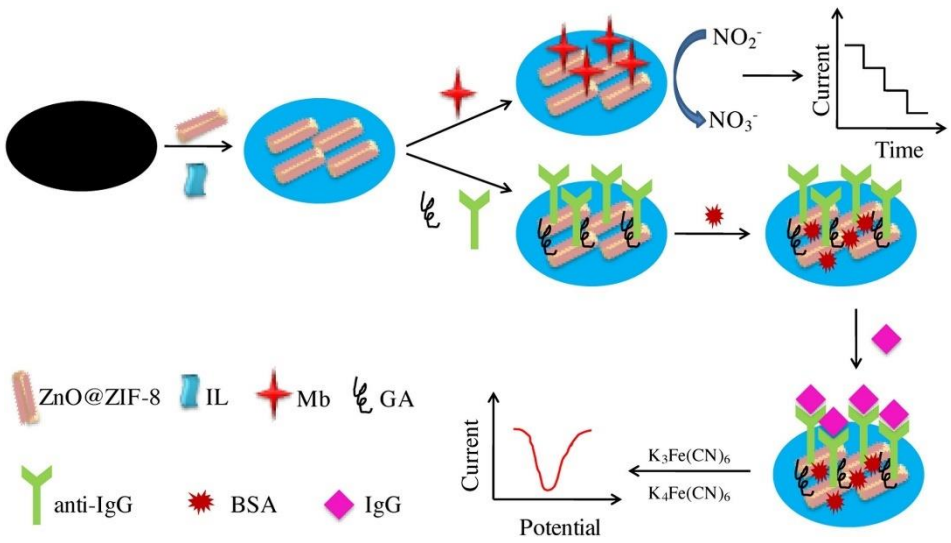

Lately, a novel synthesis of antibody orientation on MOFs has been studied (Alt et al., 2021). The crystallization of zinc-based MOFs can induce the Fc region of the antibody, where the Fc region is partially embedded within the MOF, and the Fa region protrudes. Because Zn^{2+} concentrates on negatively charged functional groups on the surface of biomacromolecules, allowing another type of ZIF structure, called ZIF-C to form

rapidly; conversely, in the presence of positively charged proteins, ZIF-C did not occur the self-assembly (Maddigan et al., 2018; Qi et al., 2017).

Figure 2.6

The ZIF-8 Coating on Fe_3O_4 Particles for Antibody Fragments Immobilization

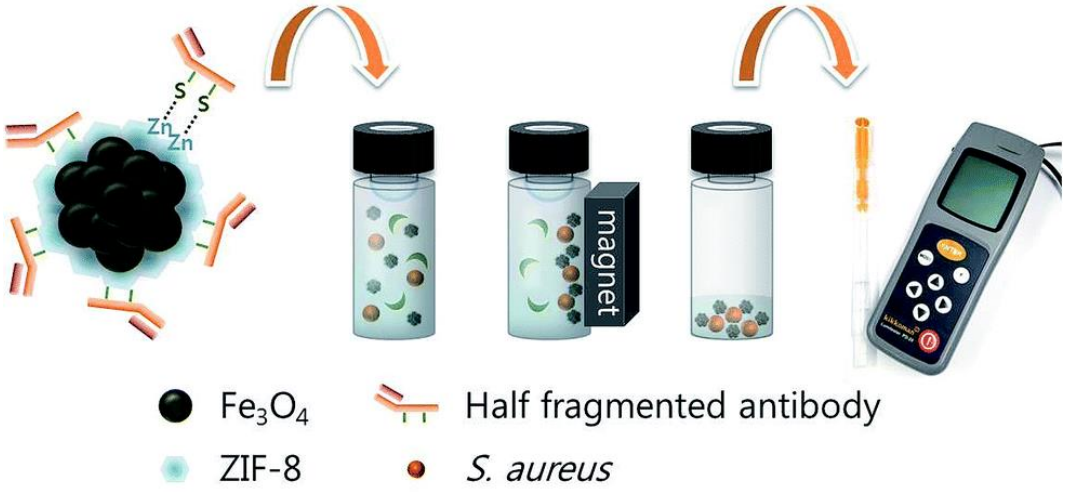

ZIF-C ($Zn_2(mIM)_2(CO_3)$) contains zinc ions, 2-mIM, and carbonate, and it is identified as a phase with different chemical and physical properties than other ZIF phases such as amorphous, diamondoid, and sodalite (P. Falcaro et al., 2020). Furthermore, CO_3^{2-} of ZIF-C is sourced from atmospheric carbon dioxide, which results in crystals with high density and stability (Basnayake et al., 2015).

Figure 2.7

The Antibody Protection Testing by Using ZIF-8 Coating

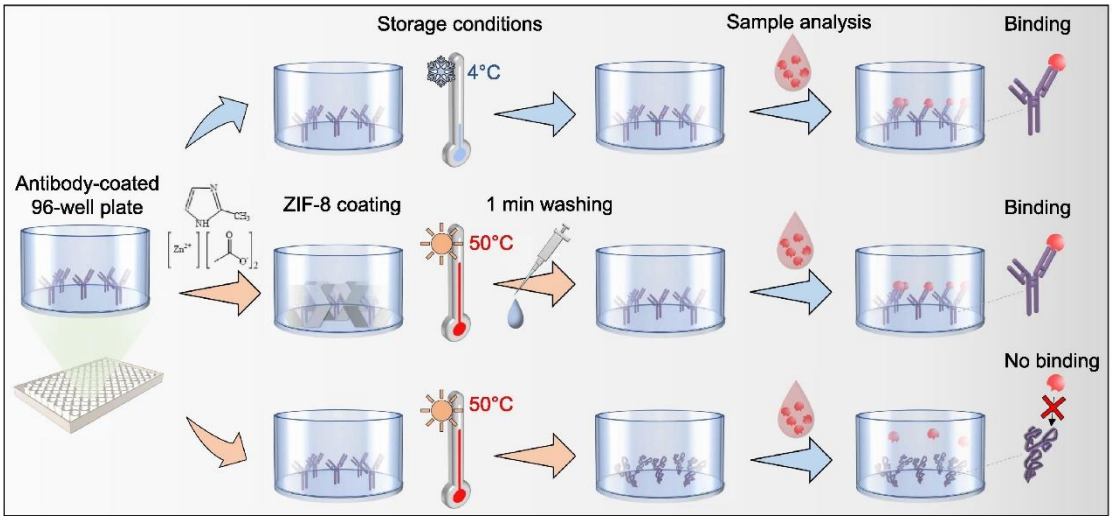

In this case, the Fab region of an antibody contains positively charged amino-terminal groups, whereas the Fc region contains negatively charged carboxyl and histidine groups (W. Zhang et al., 2020). Therefore, the immobilization of antibodies onto the MOF can induce the spatial-controlled crystallization of Zn-based ZIF around the Fc region, and thereby the orientation-controlled antibody can be inserted into the MOF particles. The final biocomposites are referred to ZIF-C*Ab, as shown in **Figure 2.8** (Alt et al., 2021). Thus, this provides a new approach for immobilizing antibodies and other biomolecules as a one-step process and heat-free synthesis.

Figure 2.8

*The Schematic of the ZIF-C*Ab Crystallization Process*

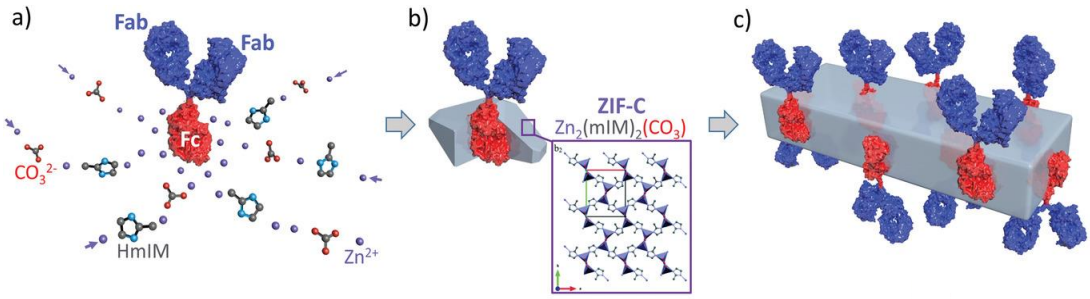

2.5 Chapter Summary

Infectious diseases, which cause epidemics such as COVID-19, influenza, and diphtheria, have a massive impact on the public health and economic systems, including on people's daily lives. Therefore, a rapid and accurate diagnosis is essential for screening and isolating infected people to prevent the spread of the disease. However, current primary assays such as real-time PCR (qPCR), enzyme-linked immunosorbent assay (ELISA), and immunomagnetic separation (IMS) for pathogen detection require state-of-the-art equipment and skilled operators, and lab operation. Therefore, these assays are not suitable for rural or home use.

Immunosensors are crucial to eliminate some limitations and allow for faster detection and a more straightforward method. Nevertheless, false negatives can occur when detecting tiny quantities of infection. Therefore, the design of the immunosensor was developed by improved antibody immobilization techniques, and nanomaterials enhanced the combined properties of transducers and biological components.

Especially, MOF-based antibody immobilization is an interesting new nanomaterial due to its high porosity, large surface area, and high chemical stability.

CHAPTER 3
METHODOLOGY

3.1 Research Diagram

The following flowchart shows the outline of the research method to achieve the objectives of this present work.

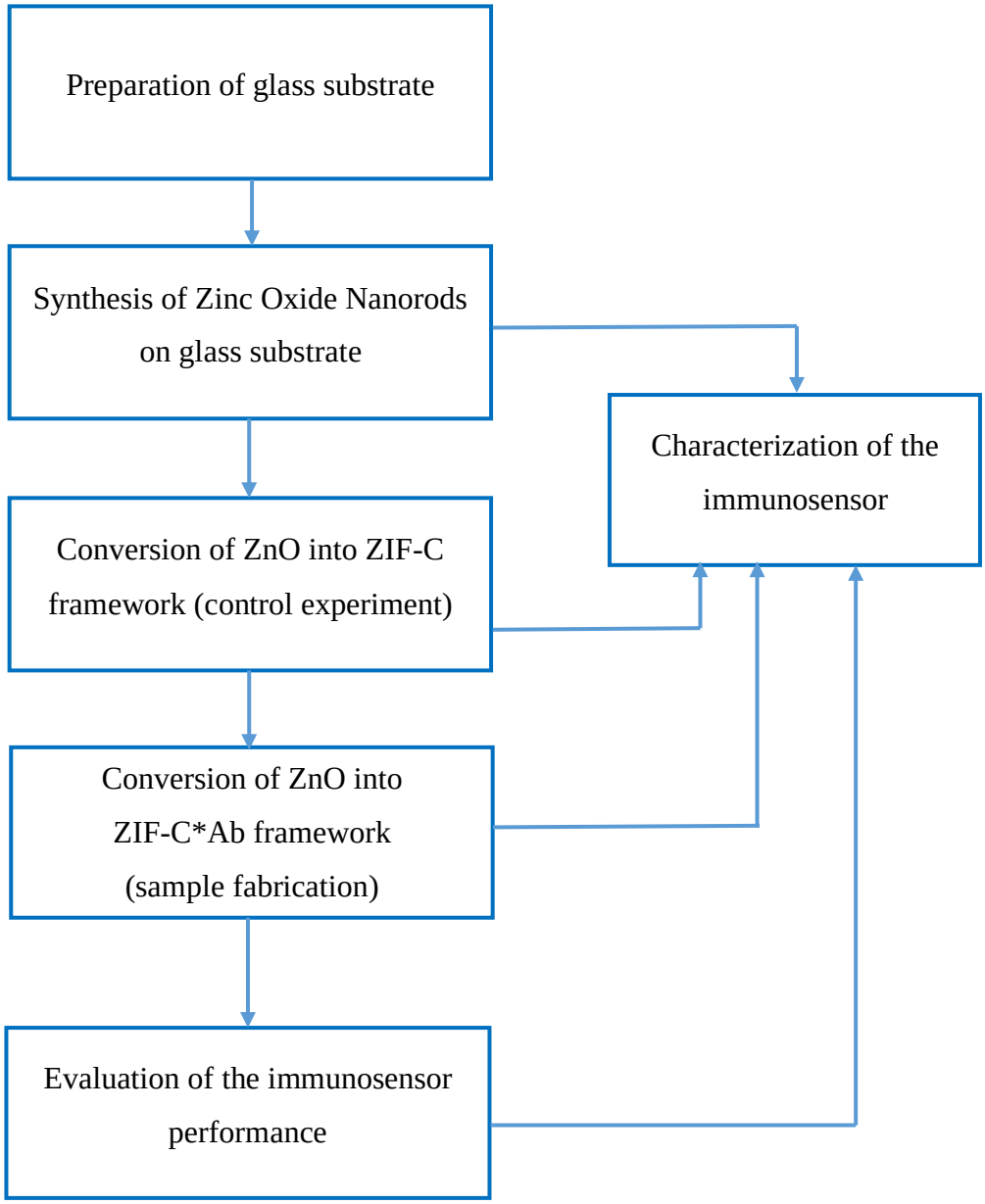

3.2 Surface Modification of Glass Substrates

3.2.1 Synthesis of Zinc Oxide Nanorods (ZnONRs) on Glass Substrates

Firstly, glass slides were cut (1x2.5 cm^2), cleaned with soap, acetone, and ethanol in a sonicator for 10 mins, and dried in an oven at 80 ˚C for 1 hour. After that, the pyrolysis spraying technique produced a zinc oxide thin film (ZnO seed) on the glass substrate. Next, the dried glass slides were placed on a hot plate at 90 ˚C and spray-coated with 10 mM of zinc acetate solution in ethanol, then annealed at 250 ˚C for 5 hours, obtaining ZnO thin film samples.

Secondly, the 30mM of ZnONRs samples were synthesized by hydrothermal growth technique. A solution was prepared with 60 mM (100 ml) of zinc nitrate hexahydrate $(Zn(NO_3)_2)\cdot 6H_2O$ and 60 mM (100 ml) of Hexamethylenetetramine (Hexamine) for growing the ZnONR on ZnO seed crystals. The samples were immersed in the mixing solution and irradiated in a microwave at 160 W (setting at minimum level) for 1 hour. After being irradiated in each cycle, the samples were washed with DI water 2-3 times and immersed in freshly made solutions and repeated in 5 cycles. After that, the samples were annealed in a furnace at 350 ˚C for 1 hour, obtaining a white layer of ZnONR on the glass substrate.

Figure 3.1

Diagram of Zno Nanorods Synthesis

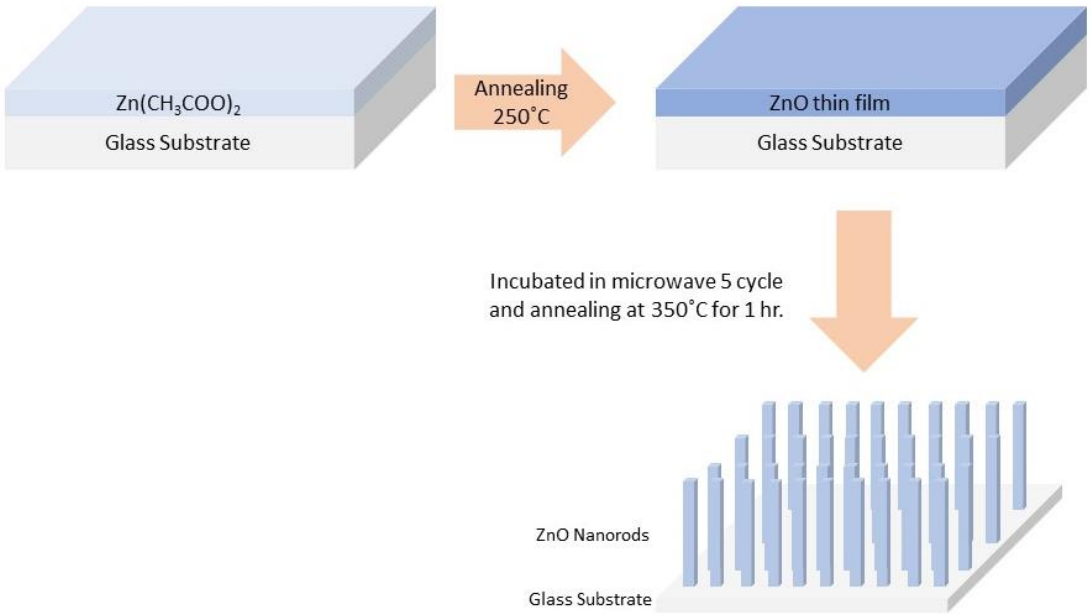

3.2.2 Conversion of ZnO into ZIF-C Framework (Control Experiment)

The conversion from ZnO to ZIF-C is performed via a simple chemical reaction. A solution of 240mM of 2-methylimidazole (HmIm) in DI water is drop-cast onto the ZnO nanorods and incubated at room temperature for 20 min. Following incubation, the converted ZIF-C substrate is washed twice with water and dried at room temperature.

Figure 3.2

The Conversion of ZnO into ZIF-C Framework of ZnO Nanorods Substrate.

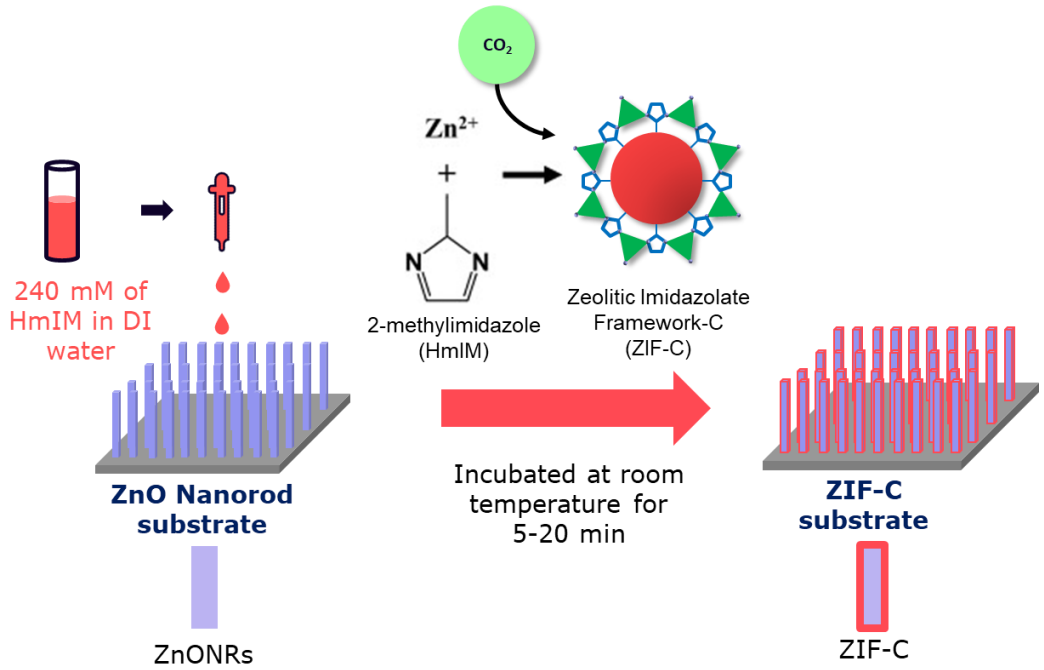

*3.2.3 Conversion of ZnO into ZIF-C*Ab Framework (Sample Fabrication)*

The same method of section 3.2.2 is followed, except for a preliminary drop cast of a 72 µg/ml solution of anti-human serum albumin antibody, followed by incubation at room temperature for 90 mins, addition of the 2-methylimidazole solution as described before. The ZIF-C*Ab substrate was washed with DI water 2-3 times to remove unbounded Ab and dried in a hood for 4 hours.

Figure 3.3

*The Conversion of ZnO into ZIF-C*Ab on the Substrate.*

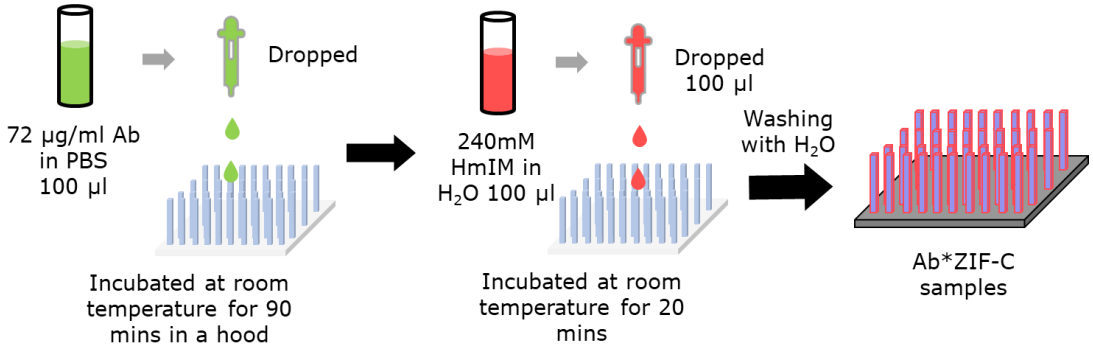

3.3 Immunosensor Performance Evaluation

3.3.1 Preparation of Fluorescein-Human Serum Albumin Solution

Fluorescein labeled-Human Serum Albumin (FL-HSA) is prepared in 50 mM of Carbonate buffer pH 8.0, at the concentrations of 5, 15, and 25 µM (1:1 molar ratio of HSA and FL). The concentration of HSA can be monitored via UV-Vis spectrophotometry at 279 nm (Abou-Zied & Sulaiman, 2014). The HSA and FL solutions were mixed and stored in the refrigerator at 4 °C overnight, which was examined by a decrease in the emission wave fluorescence intensity at 343 nm (HSA) and 521 nm (FL) when an excitation at 295 nm via fluorescent spectroscopy.

3.3.2 Sensitivity Detection Testing of the Fluorescence-based Immunosensor

After the antibody fixation on the ZIF-C surface, the sensitivity of the immunosensor was performed by analyzing the fluorescence intensity peak between the initial solution and the washed solution. Each solution concentration was dropped and left on the prepared sample for 90 minutes until dry in the hood. After that, these samples were washed with 100 ml of water, and 50 ml was taken to measure. The initial and washed solutions were diluted 10 times to a volume sufficient to perform the test via fluorescence spectroscopy with 295 nm excitation wavelength.

Figure 3.4

The Sensitive Immunosensing Evaluation with Fluorescence Spectroscopy

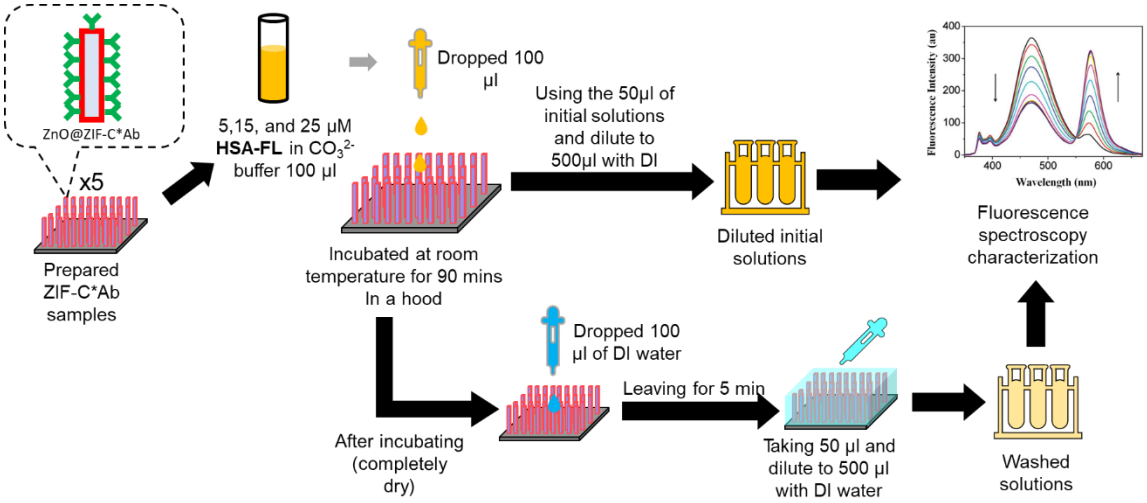

3.3.3 Selectivity Detection Testing of the Fluorescence-based Immunosensor

For the evaluation of both specific and non-specific binding on the immunosensor, 3 surfaces were analyzed: ZnO, ZIF-C, and ZIF-C*Ab. In all cases, 25 µM of HSA-FL was cast on the surface and incubated for 90 mins at room temperature in a hood. After that, samples were washed with 100 ml of water, and 50 ml was taken to measure. In the end, fluorescence spectra were collected (excitation wavelength: 295 nm), and the intensity of the peaks was analyzed to estimate the target selectivity of the sensor.

Figure 3.5

The Selective Immunosensing Evaluation

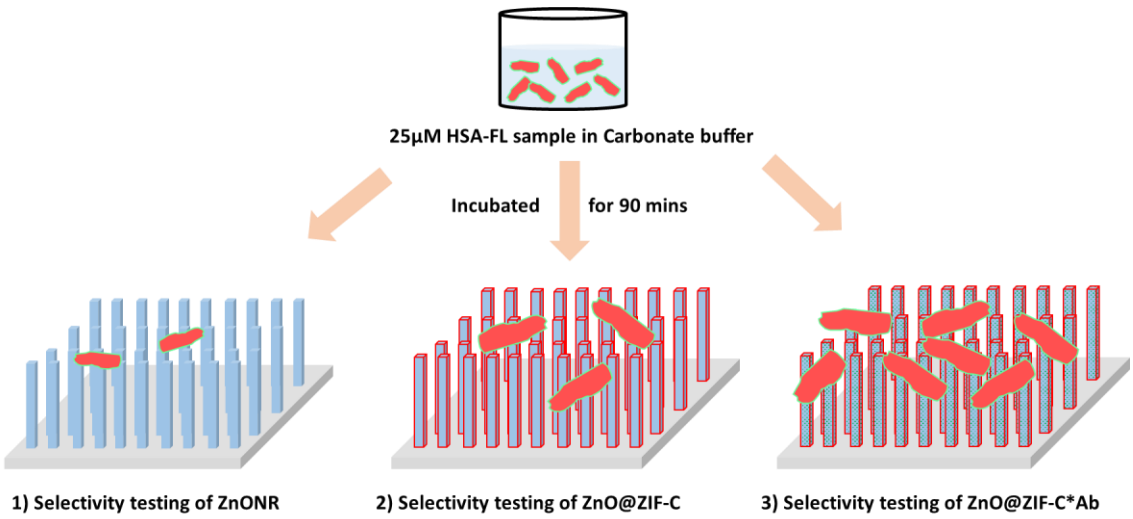

3.4 Characterization of the Immunosensor

Table 3.1

The List of Characterization Techniques

Techniques	Parameters to be evaluated
Scanning Electron Microscopy (SEM)	Surface morphology of the ZnO, ZnO@ZIF-C
UV-VIS absorption spectroscopy	Optical adsorption/Transmission of the immunosensor surface
Water Contact Angle (WCA)	Surface energy and hydrophobic/hydrophilic surface
Fourier Transform infrared spectroscopy (FTIR)	Chemical bond and functional group of Antibodies and HSA
Fluorescence spectroscopy	Fluorescence intensity of the sensing evaluation

CHAPTER 4
RESULTS AND DISCUSSION

4.1 Characterization and Morphology of ZnONR Substrates

4.1.1 Characterization of the ZnONR Structure

ZnONR Samples were synthesized with 5, 10, 15, and 30 mM of ZnONR solution via hydrothermal technique on glass substrates. These samples were characterized by Field Emission Scanning Electron Microscopy (FESEM) to observe their morphology and determine the diameter of different ZnONR concentrations. The hexagonal shape of nanorods can be ascertained by looking at the top view of ZnONR in **Figure 4.1**, with diameters of 50, 56, 68, and 95 nm for the syntheses conducted at 5, 10, 15, and 30 mM, respectively.

Figure 4.1

The Diameter Comparison of the a)5 mM, b)10 mM, c)15 mM, and d)30 mM of ZnONR Concentrations in SEM Characterization; e) Correlation Graph Between Concentration and ZnONR Diameter

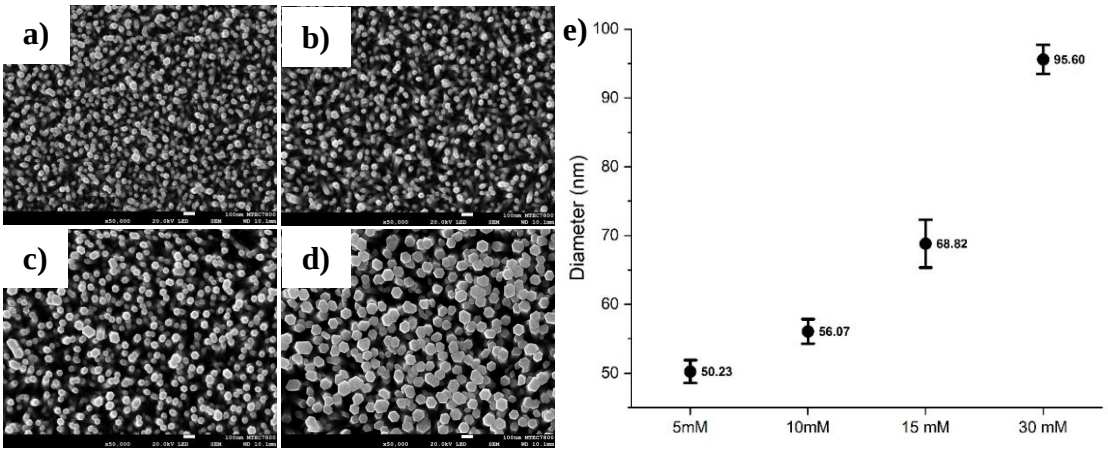

In this case, we focused on the 30 mM concentration of ZnONR since it is the optimal ratio for ZIF-C synthesis (Alt et al., 2021). According to the top view of the SEM characterization, the diameter of 30 mM ZnONR is 95 nm, as shown in **Figures 4.2a and 4.2b**. On the other hand, the cross-section view of the SEM characterization, reported in **Figure 4.2c**, shows that the thickness of the ZnONR layer (and, therefore, their diameter) is 1 µm.

Figure 4.2

The Morphology of ZnONR in a) the Top View and b) Diameter Histogram, and c) Cross-section View

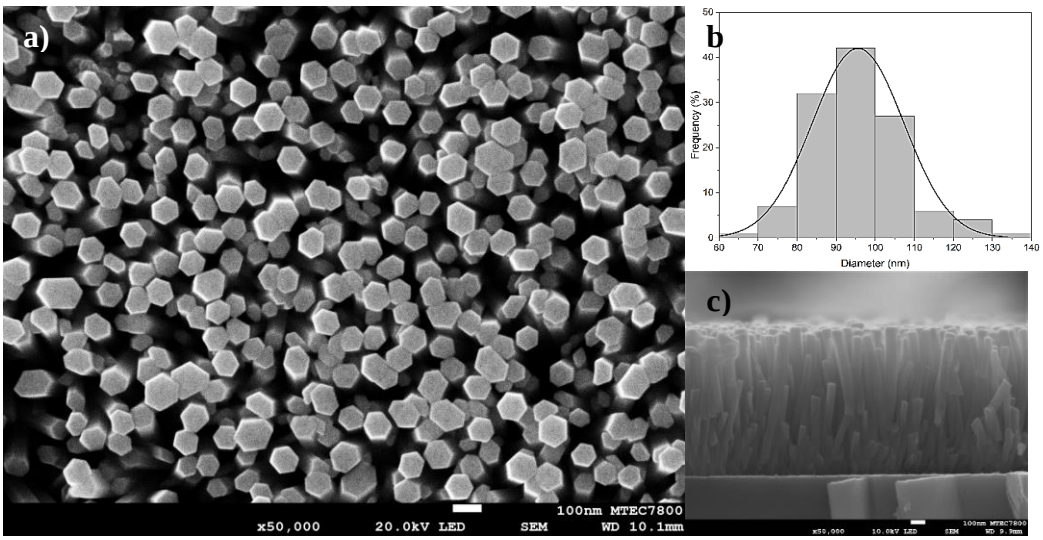

4.1.2 UV-Visible Spectroscopy Characterization of the ZnONR

According to the UV-Visible absorbance result of ZnONR shown in **Figure 4.3**, the strong absorption of the nanorods is 400 nm. There is a significant difference in absorption range compared with glass slides alone. ZnO is an excellent semiconductor with an energy band gap of 3.37eV, which resists electron-hole pair aggregation and increases photocatalytic activity, affecting light absorption as mentioned above. (Meenakshi & Sivasamy, 2017; Ramachandran et al., 2013).

Figure 4.3

UV-Visible Spectrum of ZnONR

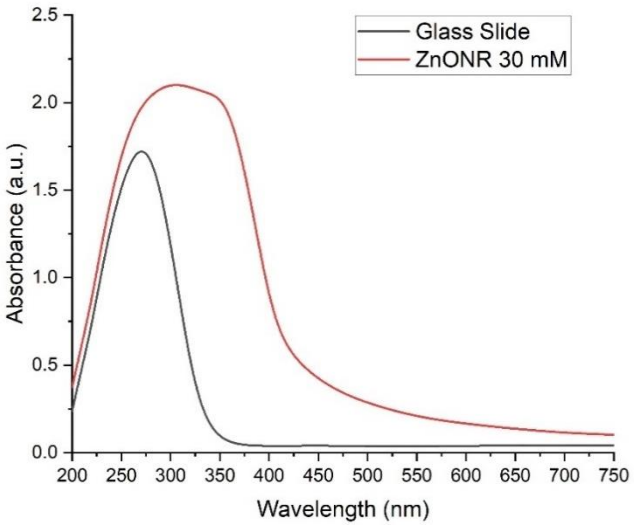

4.2 Characterization of ZnONR to ZIF-C Conversion

4.2.1 Transformation of ZnONR to ZIF-C Structure

After ZnONR synthesis, the ZnONR is converted into ZIF-C according to the chemical reaction shown below as **Equation 1.** The reaction occurs in 20 minutes (Alt et al., 2021). ZIF-C's structure and optical absorption properties were assessed by SEM, UV-Visible, and water contact angle (WCA) characterization. The SEM top view reported in **Figure 4.4a** shows that the reaction between 30 mM of Zn^{2+} and 240 mM of HmIm produces the ZIF-C structure from the conversion of the ZnO nanorods on the top half of the rod. After the reaction, the average overall diameter was increased to 201 ± 16 nm, while the diameter of the ZnO nanorod was reduced to 50 ± 8 nm.

$$ZnO + 2HmIm \xrightarrow{atmospheric\ CO_2} Zn_2(mim)_2(CO_3) + H_2O \quad (1)$$

Figure 4.4

The SEM Characterization of ZIF-C Structures on ZnONR in the a) Top-view and b) Cross-section

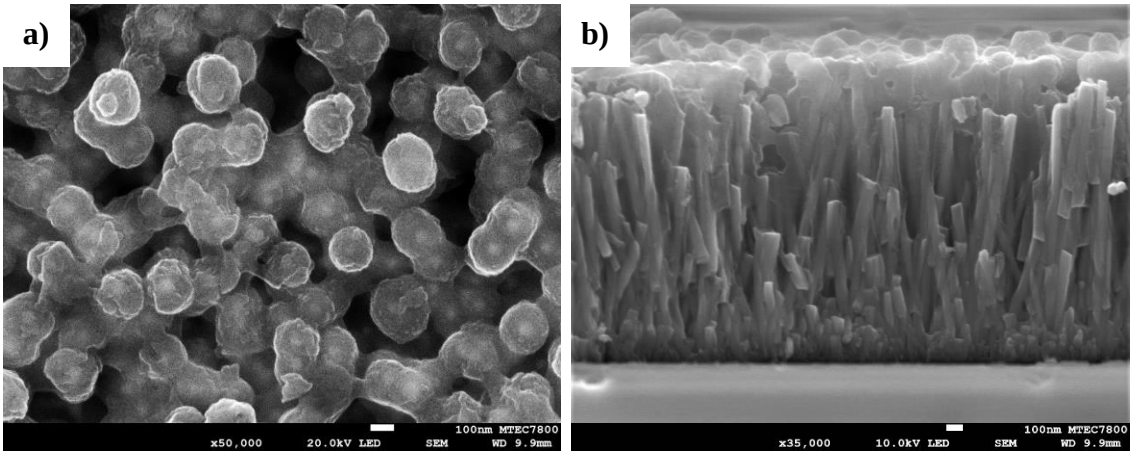

The cross-section view of the SEM shows that ZIF-C densely covered the top surface and resulted in a significant increase in thickness and length with an average overall thickness of 1.8 µm, as shown in **Figure 4.4b**. In addition, ZIF-C samples were examined by UV-Visible spectroscopy, offering a broader absorbance range than ZnONR, as shown in **Figure 4.5a**.

From the water contact angle (WCA) measurement on the ZnONR samples, we found that the surface was super hydrophilicity, with an angle of $24^{\circ} \pm 2^{\circ}$. The solid thin layers or nanorods formed by ZnO nano seeds deposited on the glass surface covering more

than 60% of the substrate are naturally hydrophilic, which is explained by the Hemiwicking condition in which water penetrates the intercostal spaces of nanorods (Myint et al., 2013). Hemiwicking is a phenomenon associated with liquid spreading on a rough hydrophilic surface due to capillary action and permeability (Krishnan et al., 2019). A significant change was observed upon conversion to ZIF-C, as shown in **Figure 4.5b.** The water contact angle increased from 24˚ to 104˚, an increment due to the modification of the surface from super hydrophilic (ZnO) to hydrophobic (ZIF-C), consistent with the SEM results.

Figure 4.5

a) The UV-Visible Absorbance Spectrum in Different Layers and b) Water Contact Angle Measurement of ZnONR and ZIF-C

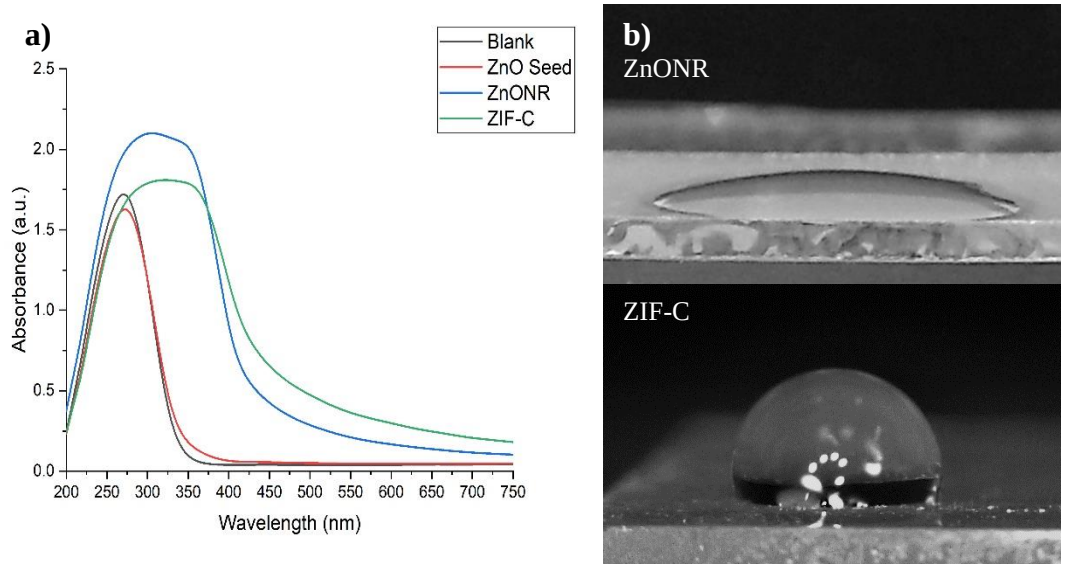

4.2.2 Optimization of Variables: Time, Concentration, Buffer Composition

This section examines the factors of reaction time, HmIm concentrations, and buffer composition that influence the conversion of ZIF-C. WCA was used to analyze the relationship between reaction conditions and surface characteristics quickly. Firstly, HmIm conversion solution was prepared in DI water at different concentrations of 120, 180, 240, 300, and 360 mM and was dripped onto the 30 mM of ZnONR sample, resulting in a metal/ligand molar ratio of 1:4, 1:6, 1:8, 1:10, and 1:12, respectively. Then, after stirring for 20 mins at room temperature, the samples were measured by WCA (**Figure 4.6)**. The graph shows that at the HmIm concentration of 240 mM, the highest degree angle was measured (ca. 104˚), thus indicating that the 1:8 metal/ligand

ratio is optimal for the conversion. This is also consistent with previous literature reports (Alt et al., 2021; Beh et al., 2018).

Figure 4.6

The Water Contact Angle Measurement of ZIF-C, Synthesized with Different HmIm Concentrations

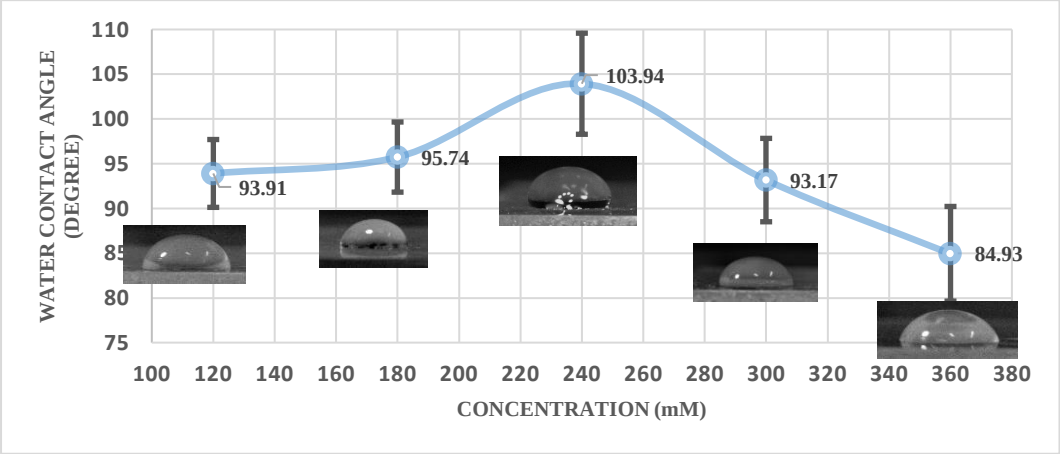

Secondly, to study the optimal reaction time for ZnO-to-ZIF-C surface conversion, samples were tested by casting 100 µl of 240 mM HmIm onto ZnONR substrates and incubating at different times, as shown in **Figure 4.7**. During the first 5 minutes, the sample surface significantly changes from a super hydrophilic surface to a more hydrophobic surface, passing from ca. 26˚ to ca. 94˚. After 10 min, a further increment of water contact angle was observed, up to a steady value of ca. 103˚, thus indicating the end of the reaction of the ZIF-C conversion. Therefore, 20 minutes of reaction time were chosen for the maximum conversion possible on the surface.

Lastly, additional methods were tested to study the effect of buffer on the ZIF-C conversion, as reported in Section 3.2.2. Since the antibodies were dissolved in 10 mM Phosphate Buffered Saline (PBS) buffer at pH 7.4, the samples needed to be tested with a pretreatment first due to the lower stability of the ZIF class of materials at this pH (De J. Velásquez-Hernández et al., 2019).

Figure 4.7

The Time Conversion of ZIF-C on ZnONR Surface Monitored via WCA

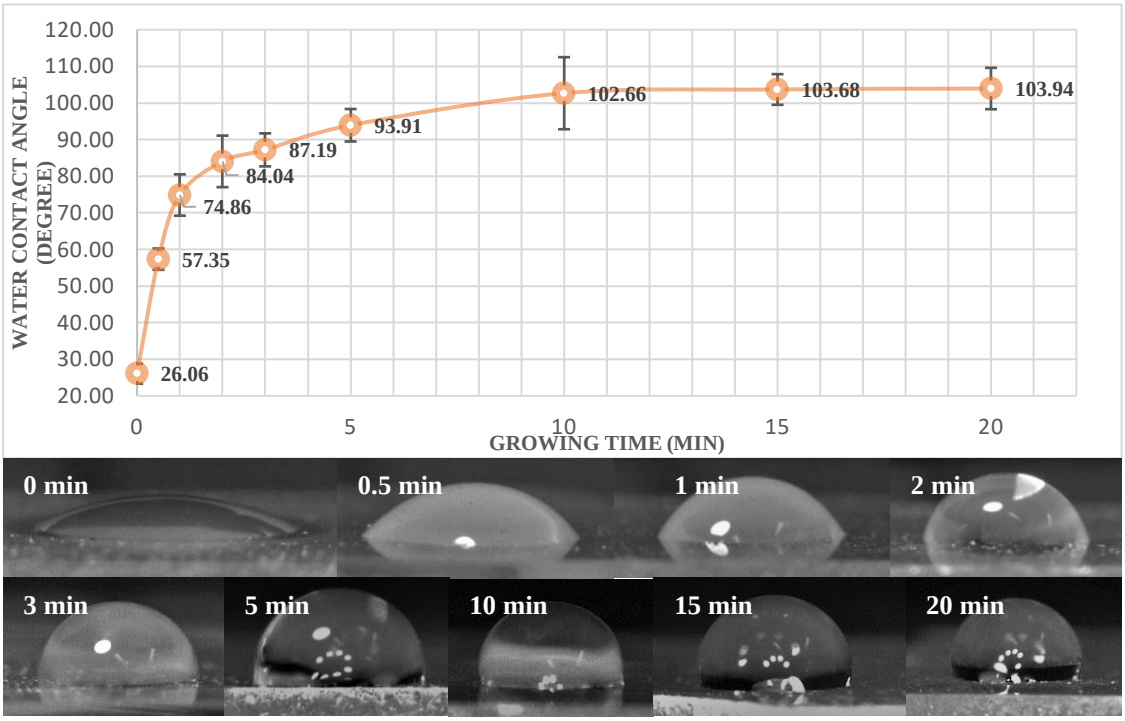

The pretreatment is a control experiment simulating the utilization of the antibody in the related buffer without its presence. Washing is then necessary to remove excess unbound antibodies. Herein, PBS and 3-(N-morpholino)propanesulfonic acid (MOPS) buffers at 10 mM pH 7.1 are used for pretreatment and washing. DI water is also used for washing, but not in the pretreatment as the antibody is necessarily dissolved in a buffer. The samples were tested in 4 ways:

Sample	***#1***	***#2***	***#3***	***#4***
Pretreatment	MOPS Buffer	MOPS Buffer	PBS Buffer	PBS Buffer
Washing	DI Water	DI Water	PBS Buffer	PBS Buffer

WCA measurements reported in **Figure 4.8** show that DI water produces the highest surface angles regardless of the pretreatment buffer, although slightly lower than the WCA right after ZIF-C conversion. This indicates a partial degradation even in mild

conditions, which is reasonable considering DI water is also slightly acidic upon exposure to air (due to dissolved CO_2).

Figure 4.8

The ZIF-C Conversion Approach in Different Buffers (Pretreatment/Washing)

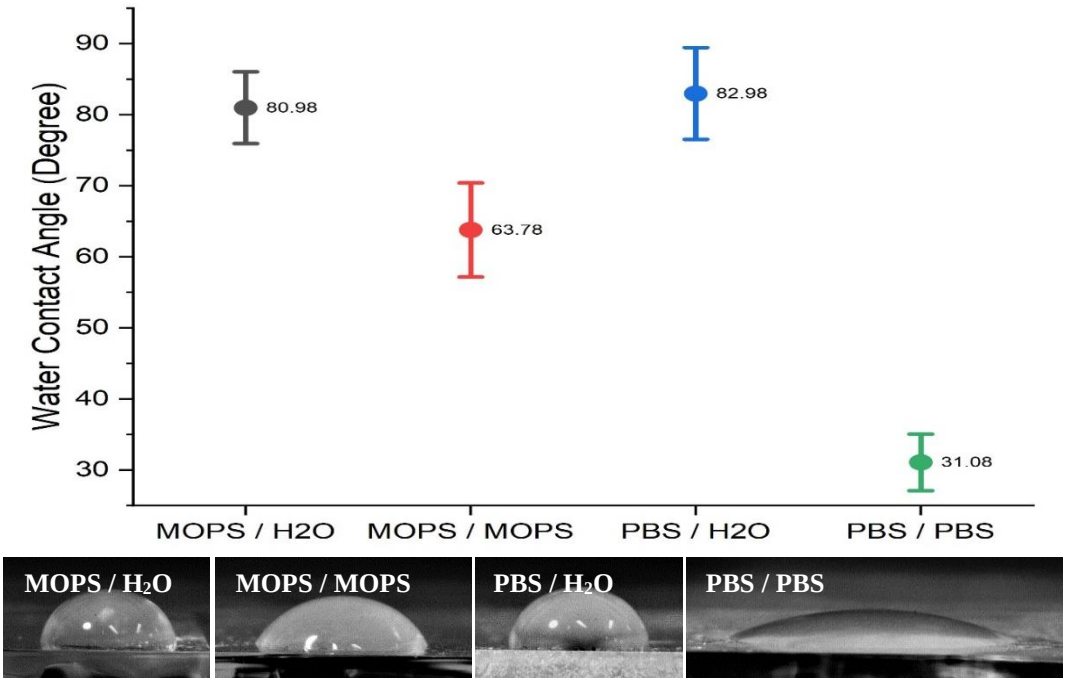

Furthermore, the MOPS buffer washing further affects the ZIF-C structure, indicating more erosion than the DI water wash. Conversely, pretreatment and washing with PBS buffer significantly affect the ZIF-C conversion, as shown by the drastically lowest water contact angle, confirming that PBS is detrimental to ZIF-C (De J. Velásquez-Hernández et al., 2019).

4.3 Conversion of ZnONR to ZIF-C*Ab

This technique's immobilization of the Anti-Human Serum Albumin monoclonal antibody (Ab) relies on the formation of MOFs surrounding the Fc region of the antibody, similar to the reinforced concrete. ZIF-C*Ab samples significantly differed from ZIF-C samples due to the protrusion of amine groups of the antibodies, resulting in more excellent hydrophilicity on the sample surface. From the water contact angle measurement in **Figure 4.9**, the sample with the antibody had a reduced angle of 58.4˚, indicating the above assumption. Additionally, when the human serum albumin (HSA) solution was dropped on the ZIF-C*Ab sample, the angle was significantly reduced to 33.67˚.

Figure 4.9

The Water Contact Angle Measurement of Different Sample Layers

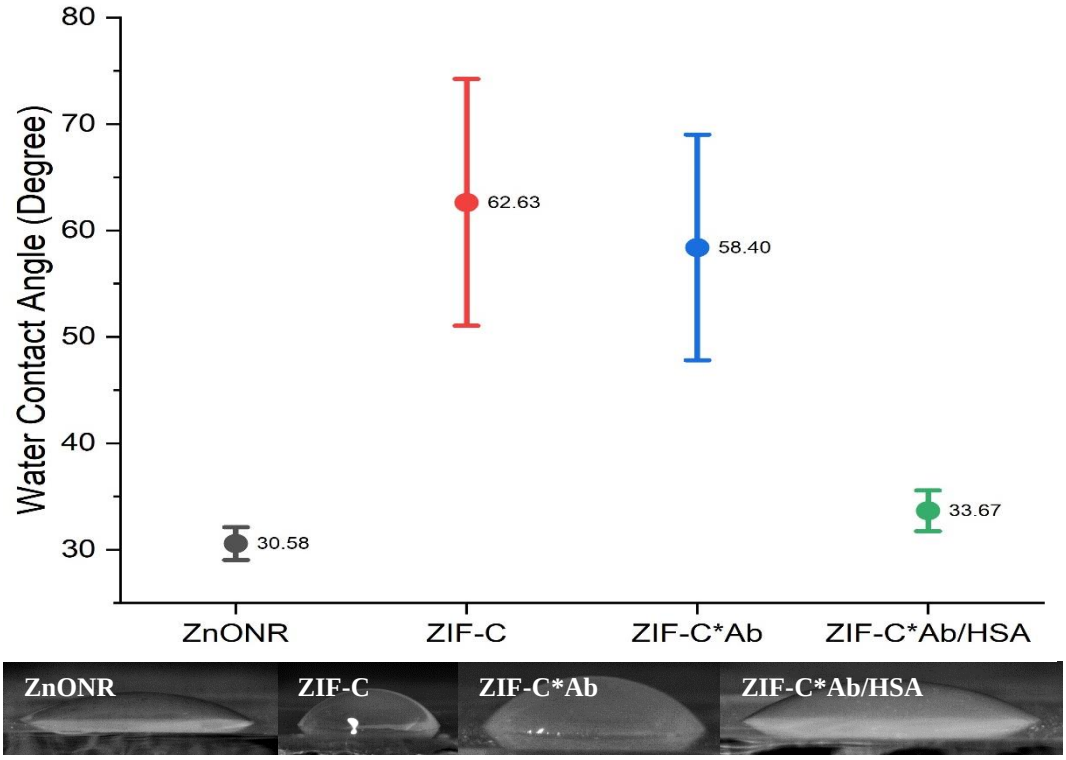

To assay antibodies in ZIF-C*Ab samples, including HSA, Fourier transforms infrared (FTIR) spectroscopy was used to examine the presence of these biological components and the ZIF-C composition on the substrate, as shown in **Figure 4.10**. Absorbance peaks indicate characteristic vibrational mode spectra of ZIF-C in the 700-850 and 1300-1600 cm^{-1} ranges, defined as the 875 cm^{-1} is the bending mode and the 1375 and 1552 cm^{-1} are the asymmetric stretching modes of CO_3^{2-}, and antibody peptide backbone, which are amide I and amide II, are 1650 cm^{-1} and 1540 cm^{-1}, respectively (Basnayake et al., 2015; Falcaro et al., 2020; Han et al., 2014; Hu et al., 2011).

Figure 4.10

*The FTIR Spectra of ZIF-C, ZIF-C*Ab, and ZIF-C*Ab/HSA*

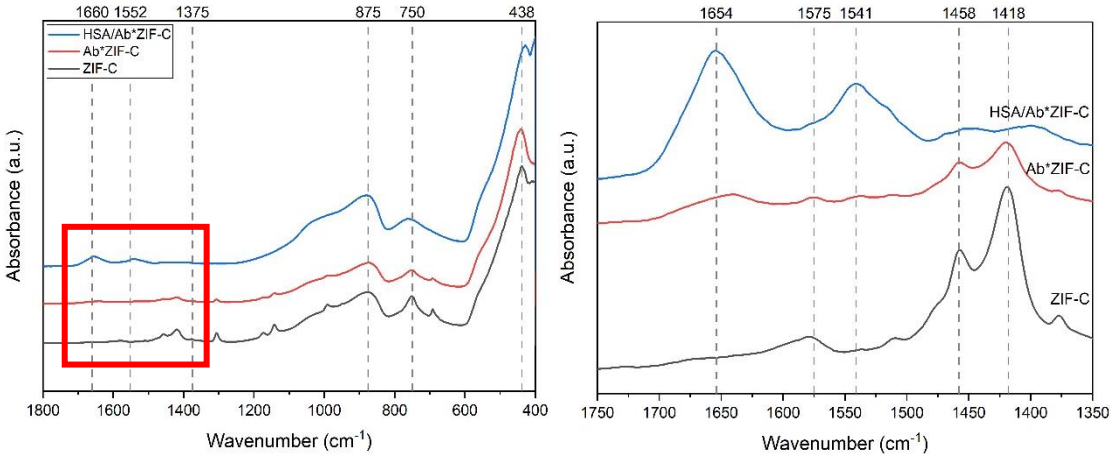

4.4 The Detection of Human Serum Albumin (HSA) and Evaluation of Antibody Immobilization

Immunosensor was examined for the detection efficiency, sensitivity, specificity, and antibody immobilization by using HSA instead of an infectious disease biomarker due to laboratory limitations. Human serum albumin was measured the fluorescence intensity of the emission wave at 343 nm by excitation at 295 nm of fluorescent spectroscopy. In addition, FL was mixed with 50 mM HSA at pH 8.0 of carbonate buffer to increase the fluorescence intensity signal, enabling further observation of the peak of FL at 521nm. However, after HSA-FL mixing, the fluorescence intensity was slightly quenched due to the binding between the carboxyl group of FL and the amine group of HSA, as shown in **Figure 4.11**.

Figure 4.11

The Fluorescence Spectra of before and after HSA-FL Mixing

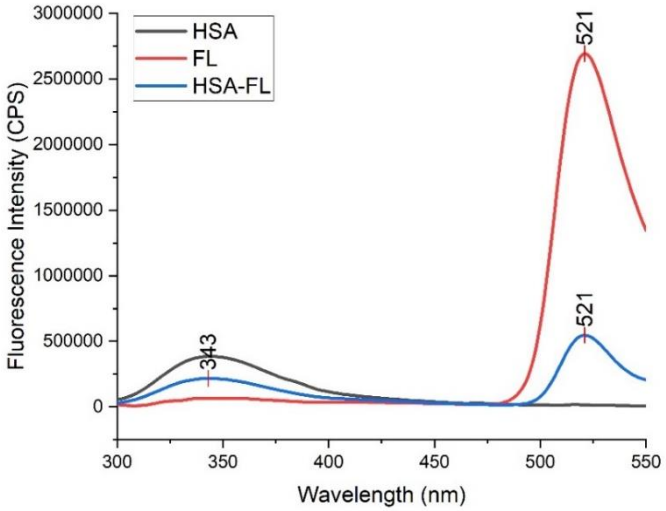

4.4.1 Testing of Specific and Non-specific Binding

The detection specificity of the immunosensor (25 µM) relies on HSA fluorescence to evaluate the capturing ability of antibodies on the sample. This experiment demonstrated the difference between samples with and without 0.72mg/ml antibodies by the HSA fluorescence on ZnO, ZIF-C and ZIF-C*Ab samples, as shown in **Figures 4.12a, 4.12b, and 4.13c**, respectively. The fluorescence intensity of each sample washed solution was measured with fluorescence spectroscopy at 295nm excitation and compared with the initial solution, approximating the amount of HSA on samples. Due to the HSA fluorescence at 343 nm, the fluorescence intensity of the initial solution subtracted from the washed solution is shown in **Figure 4.12d**, in which the ZIF-C*Ab had the highest fluorescence intensity. Therefore, the antibody is vital in helping increase the binding of HSA on the sensor surface.

4.4.2 Sensitivity of HSA Detection

The relationship between fluorescence intensity and HSA concentration was determined by the Beer-Lambert law according to the equation below:

$$FL = \varepsilon cl$$

Where FL is the fluorescence intensity, ε is the molar absorption coefficient ($M^{-1}\,cm^{-1}$), c is the molar concentration (M), and l is the optical path length (cm) that is typically 1 cm of the cuvette length.

Figure 4.12

The Evaluation of Specific and Non-specific Binding to HSA

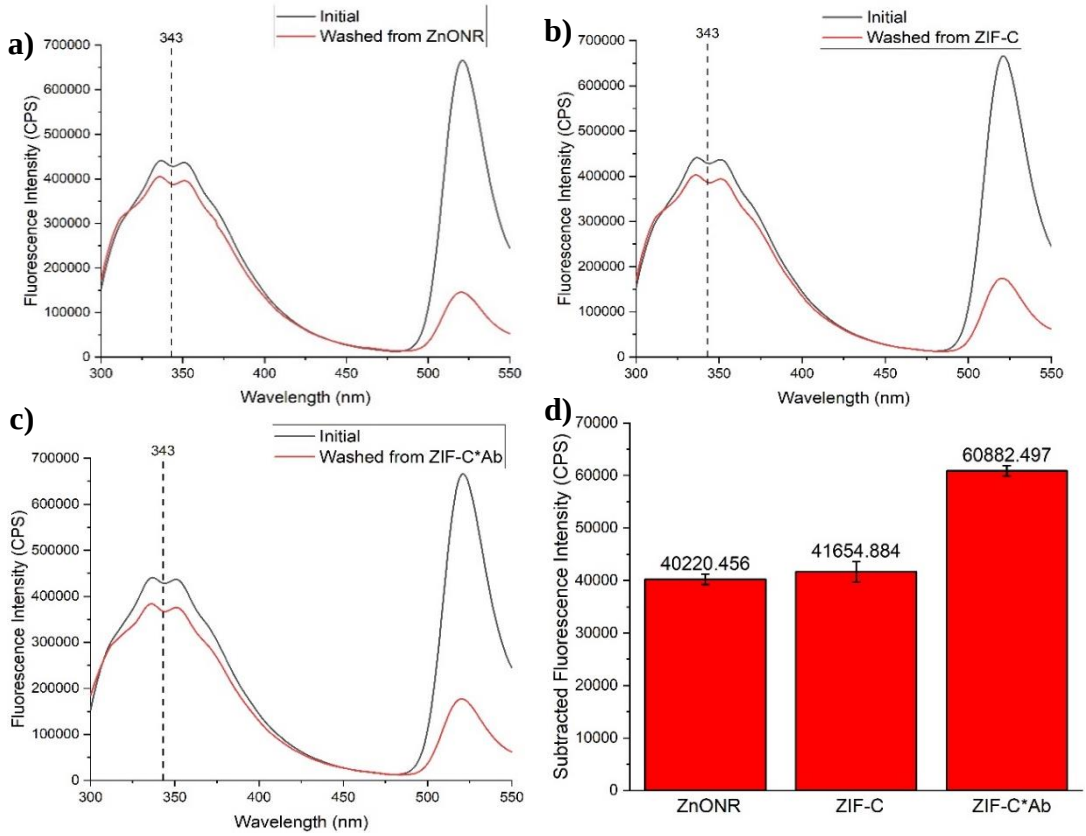

In this case, the fluorescence coefficient can be obtained from the slope of the concentration-fluorescence intensity graph at 343 nm, as shown in **Figure 4.13**. Therefore,

$$\varepsilon = \frac{FL}{cl}$$

From the slope (FL/c) is 0.0332 M^{-1} and l is 1 cm, ε is equal to 0.0332 M^{-1} cm^{-1}.

To evaluate the sensitivity of the immunosensor detection, (0.72 mg/ml) antibody samples were tested for different HSA concentrations (5, 15, and 25 µM), as shown in **Figure 4.14**. The samples were measured using the same method as the specificity test, based on the difference in the fluorescence intensity of the initial HSA solution and the washed HSA solution of each concentration.

Figure 4.13

The Relationship between HSA-FL Concentration and Fluorescence Intensity

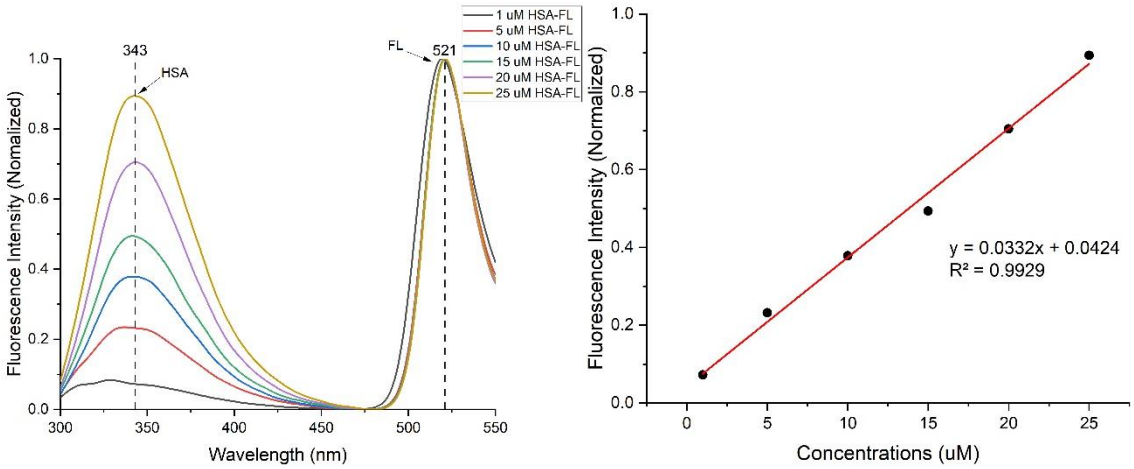

The result is a quantitative approximation of HSA, which shows significant linearity, with the slope of the linear equation yielding a constant sensitivity of 0.0288 and a LOD of 2.42 µM calculated from: $LOD = 3.3SD/S$ where SD is standard deviation and S is a slope.

Figure 4.14

The Immunosensor Sensitivity of HSA Detection

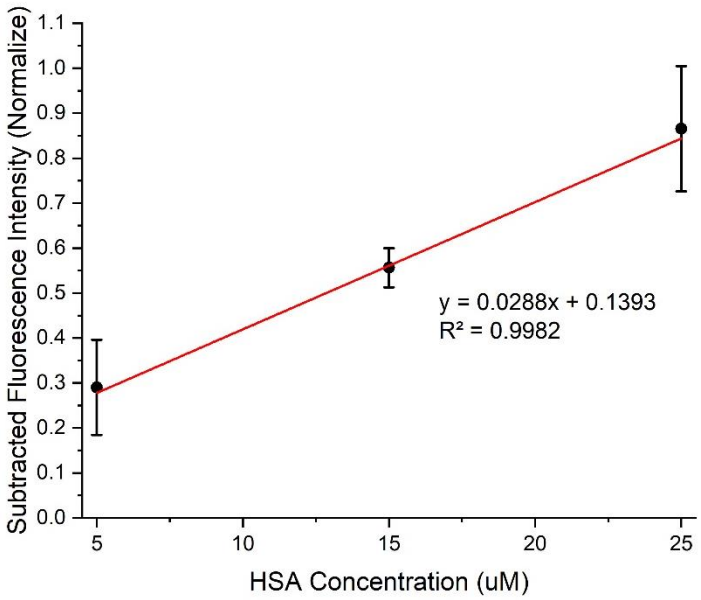

CHAPTER 5
CONCLUSION AND RECOMMENDATIONS

5.1 Conclusion

In conclusion, the fluorescent immunosensor was developed with a novel technique based on MOF materials to immobilize antibodies on the sensor surface. ZnO nanorods were vertically synthesized on glass slides via the hydrothermal method and partially converted to ZIF-C on top of ZnONR for self-assembly-oriented antibody immobilization. It is noteworthy that this is the first known example of direct conversion of ZnO into a ZIF-based poruse material conducted directly on a surface rather than in solution, as well as the first successful direct immobilization of antibodies on a surface conducted in this way. FESEM images demonstrated the hexagonal morphology of ZnONR, which has a diameter (50.2, 56.1, 68.8, and 95.6 nm) and enlarged according to the concentration (5, 10, 15, and 30 mM) of ZnONR solution used in the synthesis. For the ZnO to ZIF-C conversion, three factors: reaction time, buffer type and pH, and the concentration ratio between Zn^{2+} and HmIm, are observed from the water contact angle measurement due to the change from the super hydrophilicity (ZnO) to hydrophobicity (ZIF-C). Therefore, the optimal factors for the ZIF-C conversion are the reaction time of 10 min, the dissolved HmIm in water, and the 1:8 ratio of Zn2+:HmIm. Additionally, the UV-Vis spectra demonstrate a broader absorbance range of ZIF-C compared to ZnONR.

The challenge for antibody immobilization is the effect of PBS buffer on ZIF-C crystal degradation. We found that ZIF-C needed to react in water and keep it in the pH 7-8 range to maintain the ZIF-C crystal structure. In the HSA detection assay, the binding specificity test indicated a significantly better HSA-capturing efficiency of the ZIF-C*Ab sample, proving successful in immobilizing the antibody on the sample. Finally, the sensitivity test shows linearity between fluorescence intensity and HSA concentration, with a sensitivity of 0.0288 and a LOD of 2.42 µM.

5.2 Recommendation

In this study, we focused on novel antibody immobilization with MOF material, which has not been studied much in this area. This technique has the potential for immobilization or encapsulation of other bio-compositions such as protein, virus, DNA,

and enzyme due to its simple, fast, and non-heating process. However, in measuring actual samples with various factors such as temperature, pH, and organic solvents, it remains a challenge for this technique with great opportunities to explore and research to improve its detection potential. Therefore, in the application with other types of sensors such as SPR, electrochemical, and magnetic sensors, the immobilization MOF material also needs to be inspected and tested for electrical, optical, and thermal properties.

REFERENCES

Abou-Zied, O. K., & Sulaiman, S. A. J. (2014). Site-specific recognition of fluorescein by human serum albumin: A steady-state and time-resolved spectroscopic study. *Dyes and Pigments*, *110*, 89–96. https://doi.org/10.1016/j.dyepig.2014.05.005

Alt, K., Carraro, F., Jap, E., Linares-Moreau, M., Ricco, R., Righetto, M., Bogar, M., Amenitsch, H., Hashad, R., Doonan, C. J., Caruso, F., Hagemeyer, C. E., & Falcaro, P. (2021). Self-Assembly of Orientated Antibody-Decorated Metal-Organic Framework Nanocrystals for Active Targeting Applications. *Metal-Organic Framework*. https://doi.org/10.1002/adma.202106607

Anna MacDonald. (2020, April 6). *Developing Antibodies and Antigens for COVID-19 Diagnostics | Technology Networks*. https://www.technologynetworks.com/diagnostics/blog/developing-antibodies-and-antigens-for-covid-19-diagnostics-333088

AVRAMEAS, S., TERNYNCK, T., & GUESDON, J.-L. (1978). Coupling of Enzymes to Antibodies and Antigens. *Scandinavian Journal of Immunology*, *8*, 7–23. https://doi.org/10.1111/J.1365-3083.1978.TB03880.X

Barton, A. C., Collyer, S. D., Davis, F., Garifallou, G. Z., Tsekenis, G., Tully, E., O'Kennedy, R., Gibson, T., Millner, P. A., & Higson, S. P. J. (2009). Labeless AC impedimetric antibody-based sensors with pg ml−1 sensitivities for point-of-care biomedical applications. *Biosensors and Bioelectronics*, *24*(5), 1090–1095. https://doi.org/10.1016/J.BIOS.2008.06.001

Basnayake, S. A., Su, J., Zou, X., & Balkus, K. J. (2015). Carbonate-based zeolitic imidazolate framework for highly selective co2 capture. *Inorganic Chemistry*, *54*(4), 1816–1821. https://doi.org/10.1021/IC5027174/SUPPL_FILE/IC5027174_SI_002.CIF

Beck, O., Kraft, M., Moeller, M. R., Smith, B. L., Schneider, S., & Wennig, R. (2000). Frontline immunochromatographic device for on-site urine testing of amphetamines: laboratory validation using authentic specimens. *Annals of Clinical Biochemistry*, *37 (Pt 2)*(2), 199–204. https://doi.org/10.1258/0004563001899005

Beh, J. J., Lim, J. K., Ng, E. P., & Ooi, B. S. (2018). Synthesis and size control of zeolitic imidazolate framework-8 (ZIF-8): From the perspective of reaction kinetics and thermodynamics of nucleation. *Materials Chemistry and Physics*, *216*, 393–401. https://doi.org/10.1016/J.MATCHEMPHYS.2018.06.022

Bhattacharjee, S., Jang, M. S., Kwon, H. J., & Ahn, W. S. (2014). Zeolitic Imidazolate Frameworks: Synthesis, Functionalization, and Catalytic/Adsorption Applications. *Catalysis Surveys from Asia*, *18*(4), 101–127. https://doi.org/10.1007/s10563-014-9169-8

Biggs, H. M., Lu, X., Dettinger, L., Sakthivel, S., Watson, J. T., & Boktor, S. W. (2018). Adenovirus-Associated Influenza-Like Illness among College Students, Pennsylvania, USA - Volume 24, Number 11—November 2018 - Emerging Infectious Diseases journal - CDC. *Emerging Infectious Diseases*, *24*(11), 2117–2119. https://doi.org/10.3201/EID2411.180488

BioExplorer.net. (2019, December 13). *Types of Antibodies in Blood | Properties, Structures & Functions*. https://www.bioexplorer.net/types-of-antibodies .html/

Brena, B., González-Pombo, P., & Batista-Viera, F. (2013). Immobilization of Enzymes: A Literature Survey. *Methods in Molecular Biology*, *1051*, 15–31. https://doi.org/10.1007/978-1-62703-550-7_2

Brückner, M., Simon, J., Landfester, K., & Mailänder, V. (2021). The conjugation strategy affects antibody orientation and targeting properties of nanocarriers. *Nanoscale*, *13*(21), 9816–9824. https://doi.org/10.1039/D0NR08191D

Cai, X., Chen, J., Hu, J., Long, Q., Deng, H., Fan, K., Liao, P., Liu, B., Wu, G., Chen, Y., Li, Z., Wang, K., Zhang, X., Tian, W., Xiang, J., Du, H., Wang, J., Hu, Y., Tang, N., … Wang, D. (2020). A Peptide-based Magnetic Chemiluminescence Enzyme Immunoassay for Serological Diagnosis of Corona Virus Disease 2019 (COVID-19). *The Journal of Infectious Diseases*, 2020.02.22.20026617. https://doi.org/10.1101/2020.02.22.20026617

Carter, L. J., Garner, L. V., Smoot, J. W., Li, Y., Zhou, Q., Saveson, C. J., Sasso, J. M., Gregg, A. C., Soares, D. J., Beskid, T. R., Jervey, S. R., & Liu, C. (2020). Assay Techniques and Test Development for COVID-19 Diagnosis. In *ACS Central Science* (Vol. 6, Issue 5, pp. 591–605). https://doi.org/10.1021 /acscentsci.0c00501

Centers for Disease Control and Prevention (CDC). (2021, February 22). *Symptoms of COVID-19 | CDC*. https://www.cdc.gov/coronavirus/2019-ncov/symptoms-testing/symptoms.html#

Centers for Disease Control and Prevention, N. C. for I. and R. D. (NCIRD). (2020, August 31). *Flu Symptoms & Diagnosis | CDC*. https://www.cdc.gov/flu/symptoms/index.html

Choi, S., & Oh, M. (2019). Well-Arranged and Confined Incorporation of PdCo Nanoparticles within a Hollow and Porous Metal–Organic Framework for Superior Catalytic Activity. *Angewandte Chemie International Edition*, *58*(3), 866–871. https://doi.org/10.1002/ANIE.201812827

Conroy, P. J., Hearty, S., Leonard, P., & O'Kennedy, R. J. (2009). Antibody production, design and use for biosensor-based applications. *Seminars in Cell & Developmental Biology*, *20*(1), 10–26. https://doi.org/10.1016/J.SEMCDB.2009.01.010

Cristea, C., Florea, A., Tertiș, M., & Săndulescu, R. (2015). Immunosensors. *Biosensors - Micro and Nanoscale Applications*. https://doi.org/10.5772/60524

Daniels, J. S., & Pourmand, N. (2007). Label-Free Impedance Biosensors: Opportunities and Challenges. *Electroanalysis*, *19*(12), 1239. https://doi.org/10.1002/ELAN.200603855

De J. Velásquez-Hernández, M., Ricco, R., Carraro, F., Limpoco, F. T., Linares-Moreau, M., Leitner, E., Wiltsche, H., Rattenberger, J., Schröttner, H., Frühwirt, P., Stadler, E. M., Gescheidt, G., Amenitsch, H., Doonan, C. J., & Falcaro, P. (2019). Degradation of ZIF-8 in phosphate buffered saline media. *CrystEngComm*, *21*(31), 4538–4544. https://doi.org/10.1039/C9CE00757A

De Juan-Franco, E. de, Caruz, A., Pedrajas, J. R., & Lechuga, L. M. (2013). Site-directed antibody immobilization using a protein A–gold binding domain fusion protein for enhanced SPR immunosensing. *Analyst*, *138*(7), 2023–2031. https://doi.org/10.1039/C3AN36498D

Dong, S., Tong, M., Zhang, D., & Huang, T. (2017). The strategy of nitrite and immunoassay human IgG biosensors based on ZnO@ZIF-8 and ionic liquid composite film. *Sensors and Actuators, B: Chemical*, *251*, 650–657. https://doi.org/10.1016/j.snb.2017.05.047

Doonan, C., Riccò, R., Liang, K., Bradshaw, D., & Falcaro, P. (2017). Metal–Organic Frameworks at the Biointerface: Synthetic Strategies and Applications. *Accounts of Chemical Research*, *50*(6), 1423–1432. https://doi.org/10.1021/ACS.ACCOUNTS.7B00090

Engvall, E., & Perlmann, P. (1971). Enzyme-linked immunosorbent assay (ELISA) quantitative assay of immunoglobulin G. *Immunochemistry*, *8*(9), 871–874. https://doi.org/10.1016/0019-2791(71)90454-X

Falcaro, P., Carraro, F., Velásquez-Hernández, M. D. J., Astria, E., Liang, W., Twight, L., Parise, C., Ge, M., Huang, Z., Ricco, R., Zou, X., Villanova, L., Kappe, C. O., & Doonan, C. (2020). Phase dependent encapsulation and release profile of ZIF-based biocomposites. *Chemical Science*, *11*(13), 3397–3404. https://doi.org/10.1039/C9SC05433B

Falcaro, Paolo, Ricco, R., Yazdi, A., Imaz, I., Furukawa, S., Maspoch, D., Ameloot, R., Evans, J. D., & Doonan, C. J. (2016). Application of metal and metal oxide nanoparticles at MOFs. *Coordination Chemistry Reviews*, *307*, 237–254. https://doi.org/10.1016/j.ccr.2015.08.002

Feng, Y., Wang, H., Zhang, S., Zhao, Y., Gao, J., Zheng, Y., Zhao, P., Zhang, Z., Zaworotko, M. J., Cheng, P., Ma, S., & Chen, Y. (2019). Antibodies@MOFs: An In Vitro Protective Coating for Preparation and Storage of Biopharmaceuticals. *Advanced Materials*, *31*(2), 1805148. https://doi.org/10.1002/ADMA.201805148

Furukawa, H., Cordova, K. E., O'Keeffe, M., & Yaghi, O. M. (2013). The chemistry and applications of metal-organic frameworks. *Science*, *341*(6149). https://doi.org/10.1126/SCIENCE.1230444/SUPPL_FILE/FURUKAWA.SM.CORRECTED.PDF

Gao, S., Guisán, J. M., & Rocha-Martin, J. (2021). Oriented immobilization of antibodies onto sensing platforms - A critical review. *Analytica Chimica Acta*, *xxxx*. https://doi.org/10.1016/j.aca.2021.338907

Gkaniatsou, E., Sicard, C., Ricoux, R., Mahy, J. P., Steunou, N., & Serre, C. (2017). Metal-organic frameworks: A novel host platform for enzymatic catalysis and detection. *Materials Horizons*, *4*(1), 55–63. https://doi.org/10.1039/C6MH00312E

Han, S. J., Rathinaraj, P., Park, S. Y., Kim, Y. K., Lee, J. H., Kang, I. K., Moon, J. S., & Winiarz, J. G. (2014). Specific intracellular uptake of herceptin-conjugated CdSe/ZnS quantum dots into breast cancer cells. *BioMed Research International*, *2014*. https://doi.org/10.1155/2014/954307

Haukanes, B., & Kvam, C. (1993). Application of magnetic beads in bioassays. *Bio/Technology (Nature Publishing Company)*, *11*(1), 60–63. https://doi.org/10.1038/NBT0193-60

Hosu, O., Selvolini, G., & Marrazza, G. (2018). Recent advances of immunosensors for detecting food allergens. *Current Opinion in Electrochemistry*, *10*, 149–156. https://doi.org/10.1016/J.COELEC.2018.05.022

Hu, Y., Kazemian, H., Rohani, S., Huang, Y., & Song, Y. (2011). In situ high pressure study of ZIF-8 by FTIR spectroscopy. *Chemical Communications*, *47*(47), 12694–12696. https://doi.org/10.1039/C1CC15525C

Huo, J., Aguilera-Sigalat, J., El-Hankari, S., & Bradshaw, D. (2015). Magnetic MOF microreactors for recyclable size-selective biocatalysis. *Chemical Science*, *6*(3), 1938–1943. https://doi.org/10.1039/C4SC03367A

Ingavle, G. C., Baillie, L. W. J., Zheng, Y., Lis, E. K., Savina, I. N., Howell, C. A., Mikhalovsky, S. V., & Sandeman, S. R. (2015). Affinity binding of antibodies to supermacroporous cryogel adsorbents with immobilized protein A for removal of anthrax toxin protective antigen. *Biomaterials*, *50*(1), 140–153. https://doi.org/10.1016/J.BIOMATERIALS.2015.01.039

Iwamoto, T., Sonobe, T., & Hayashi, K. (2003). Loop-Mediated Isothermal Amplification for Direct Detection of Mycobacterium tuberculosis Complex, M. avium, and M. intracellulare in Sputum Samples. *Journal of Clinical Microbiology*, *41*(6), 2616. https://doi.org/10.1128/JCM.41.6.2616-2622.2003

James, L., Vernon, M. O., Jones, R. C., Stewart, A., Lu, X., Zollar, L. M., Chudoba, M., Westercamp, M., Alcasid, G., Duffee-Kerr, L., Wood, L., Boonlayangoor, S., Bethel, C., Ritger, K., Conover, C., Erdman, D. D., & Gerber, S. I. (2007). Outbreak of human adenovirus type 3 infection in a pediatric long-term care facility - Illinois, 2005. *Clinical Infectious Diseases*, *45*(4), 416–420. https://doi.org/10.1086/519938/2/45-4-416-FIG001.GIF

Jiang, X., Li, D., Xu, X., Ying, Y., Li, Y., Ye, Z., & Wang, J. (2008). Immunosensors for detection of pesticide residues. *Biosensors and Bioelectronics*, *23*(11), 1577–1587. https://doi.org/10.1016/J.BIOS.2008.01.035

Kalil, A. C., & Thomas, P. G. (2019). Influenza virus-related critical illness: pathophysiology and epidemiology. *Critical Care*, *23*(1). https://doi.org/10.1186/S13054-019-2539-X

Kang, L., Smith, S., & Wang, C. (2021). Stabilization of surface-bound antibodies for ELISA based on a reversable zeolitic imidazolate framework-8 coating. *Journal of Colloid and Interface Science*, *588*, 101–109. https://doi.org/10.1016/j.jcis.2020.12.068

Katti, M. K. (2001). Are Enzyme-Linked Immunosorbent Assay and Immunoblot Assay Independent in Immunodiagnosis of Infectious Diseases? *Clinical Infectious Diseases*, *32*(7), 1114–1114. https://doi.org/10.1086/319611

Kotra, L. P. (2007). Infectious Diseases. *XPharm: The Comprehensive Pharmacology Reference*, 1–2. https://doi.org/10.1016/B978-008055232-3.60849-9

Kreno, L. E., Leong, K., Farha, O. K., Allendorf, M., Duyne, R. P. Van, & Hupp, J. T. (2011). Metal–Organic Framework Materials as Chemical Sensors. *Chemical Reviews*, *112*(2), 1105–1125. https://doi.org/10.1021/CR200324T

Krishnan, S. R., Bal, J., & Putnam, S. A. (2019). A simple analytic model for predicting the wicking velocity in micropillar arrays. *Scientific Reports 2019 9:1*, *9*(1), 1–9. https://doi.org/10.1038/s41598-019-56361-7

Kurosaki, Y., Martins, D. B. G., Kimura, M., Catena, A. dos S., Borba, M. A. C. S. M., Mattos, S. da S., Abe, H., Yoshikawa, R., Filho, J. L. de L., & Yasuda, J. (2017). Development and evaluation of a rapid molecular diagnostic test for Zika virus infection by reverse transcription loop-mediated isothermal amplification. *Scientific Reports*, *7*(1). https://doi.org/10.1038/S41598-017-13836-9

Lesch, H. P., Kaikkonen, M. U., Pikkarainen, J. T., & Ylä-Herttuala, S. (2010). Avidin-biotin technology in targeted therapy. *Http://Dx.Doi.Org/10.1517/17425241003677749*, *7*(5), 551–564. https://doi.org/10.1517/17425241003677749

Li, M., Fan, D., & Wang, X. (2020). Economic and health impacts of infectious diseases in China: A protocol for systematic review and meta analysis. *Medicine*, *99*(30), e21249. https://doi.org/10.1097/MD.0000000000021249

Liang, K., Coghlan, C. J., Bell, S. G., Doonan, C., & Falcaro, P. (2015). Enzyme encapsulation in zeolitic imidazolate frameworks: a comparison between controlled co-precipitation and biomimetic mineralisation. *Chemical Communications*, *52*(3), 473–476. https://doi.org/10.1039/C5CC07577G

Liang, K., Ricco, R., Doherty, C. M., Styles, M. J., Bell, S., Kirby, N., Mudie, S., Haylock, D., Hill, A. J., Doonan, C. J., & Falcaro, P. (2015). Biomimetic mineralization of metal-organic frameworks as protective coatings for biomacromolecules. *Nature Communications 2015 6:1*, *6*(1), 1–8. https://doi.org/10.1038/ncomms8240

Liang, S. L., & Chan, D. W. (2007). Enzymes and related proteins as cancer biomarkers: A proteomic approach. *Clinica Chimica Acta*, *381*(1), 93–97. https://doi.org/10.1016/J.CCA.2007.02.017

Liang, S., Wu, X. L., Xiong, J., Zong, M. H., & Lou, W. Y. (2020). Metal-organic frameworks as novel matrices for efficient enzyme immobilization: An update review. *Coordination Chemistry Reviews*, *406*, 213149. https://doi.org/10.1016/J.CCR.2019.213149

Lisi, F., Falcaro, P., Buso, D., Hill, A. J., Barr, J. A., Crameri, G., Nguyen, T.-L., Wang, L.-F., & Mulvaney, P. (2012). Biosensors: Rapid Detection of Hendra Virus Using Magnetic Particles and Quantum Dots (Adv. Healthcare Mater. 5/2012). *Advanced Healthcare Materials*, *1*(5), 529–529. https://doi.org/10.1002/ADHM.201290022

Lou, D., Fan, L., Cui, Y., Zhu, Y., Gu, N., & Zhang, Y. (2018). Fluorescent Nanoprobes with Oriented Modified Antibodies to Improve Lateral Flow Immunoassay of Cardiac Troponin I. *Analytical Chemistry*, *90*(11), 6502–6508. https://doi.org/10.1021/ACS.ANALCHEM.7B05410

Louie, M., Louie, L., & Simor, A. E. (2000). The role of DNA amplification technology in the diagnosis of infectious diseases. *CMAJ: Canadian Medical Association Journal*, *163*(3), 301. https://doi.org/10.1016/S1381-1169(00)00220-X

Luckarift, H. R., Spain, J. C., Naik, R. R., & Stone, M. O. (2004). Enzyme immobilization in a biomimetic silica support. *Nature Biotechnology 2004 22:2*, *22*(2), 211–213. https://doi.org/10.1038/nbt931

Luppa, P. B., Sokoll, L. J., & Chan, D. W. (2001). Immunosensors—principles and applications to clinical chemistry. *Clinica Chimica Acta*, *314*(1–2), 1–26. https://doi.org/10.1016/S0009-8981(01)00629-5

Maddigan, N. K., Tarzia, A., Huang, D. M., Sumby, C. J., Bell, S. G., Falcaro, P., & Doonan, C. J. (2018). Protein surface functionalisation as a general strategy for facilitating biomimetic mineralisation of ZIF-8. *Chemical Science*, *9*(18), 4217–4223. https://doi.org/10.1039/C8SC00825F

McKinlay, A. C., Morris, R. E., Horcajada, P., Férey, G., Gref, R., Couvreur, P., & Serre, C. (2010). BioMOFs: Metal–Organic Frameworks for Biological and Medical Applications. *Angewandte Chemie International Edition*, *49*(36), 6260–6266. https://doi.org/10.1002/ANIE.201000048

Meenakshi, G., & Sivasamy, A. (2017). Synthesis and characterization of zinc oxide nanorods and its photocatalytic activities towards degradation of 2,4-D. *Ecotoxicology and Environmental Safety*, *135*, 243–251. https://doi.org/10.1016/J.ECOENV.2016.10.010

Mehta, J., Bhardwaj, N., Bhardwaj, S. K., Kim, K. H., & Deep, A. (2016). Recent advances in enzyme immobilization techniques: Metal-organic frameworks as novel substrates. *Coordination Chemistry Reviews*, *322*, 30–40. https://doi.org/10.1016/J.CCR.2016.05.007

MENON, P., KAPILA, K., & OHRI, V. (1999). POLYMERASE CHAIN REACTION AND ADVANCES IN INFECTIOUS DISEASE DIAGNOSIS. *Medical Journal, Armed Forces India*, *55*(3), 229. https://doi.org/10.1016/S0377-1237(17)30450-1

Mistry, K., Layek, K., Mahapatra, A., RoyChaudhuri, C., & Saha, H. (2014). A review on amperometric-type immunosensors based on screen-printed electrodes. *The Analyst*, *139*(10), 2289–2311. https://doi.org/10.1039/C3AN02050A

Mollarasouli, F., Kurbanoglu, S., & Ozkan, S. A. (2019). The role of electrochemical immunosensors in clinical analysis. *Biosensors*, *9*(3), 1–19. https://doi.org/10.3390/bios9030086

Moore, S. (2021, May 25). *What are Infectious Diseases?* https://www.news-medical.net/health/What-are-Infectious-Diseases.aspx

Myint, M. T. Z., Kumar, N. S., Hornyak, G. L., & Dutta, J. (2013). Hydrophobic/hydrophilic switching on zinc oxide micro-textured surface. *Applied Surface Science*, *264*, 344–348. https://doi.org/10.1016/j.apsusc.2012.10.024

National Foundation for Infectious Diseases. (2021, July). *Coronaviruses – National Foundation for Infectious Diseases*. https://www.nfid.org/infectious-diseases/coronaviruses/

Needs, P. (2018). Ocean in situ sensors: New developments in biological sensors. In *Challenges and Innovations in Ocean In Situ Sensors: Measuring Inner Ocean Processes and Health in the Digital Age*. https://doi.org/10.1016/B978-0-12-809886-8.00003-X

Ortega-Vinuesa, J., & Bastos-González, D. (2001). A review of factors affecting the performances of latex agglutination tests. *Journal of Biomaterials Science. Polymer Edition*, *12*(4), 379–408. https://doi.org/10.1163/156856201750195289

Oswald, B., Lehmann, F., Simon, L., Terpetschnig, E., & Wolfbeis, O. S. (2000). Red Laser-Induced Fluorescence Energy Transfer in an Immunosystem. *Analytical Biochemistry*, *280*(2), 272–277. https://doi.org/10.1006/ABIO.2000.4553

Otshudiema, J. O., Acosta, A. M., Cassiday, P. K., Hadler, S. C., Hariri, S., & Tiwari, T. S. P. (2020). Respiratory Illness Caused by Corynebacterium diphtheriae and C. ulcerans , and Use of Diphtheria Antitoxin in the United States, 1996–2018 . *Clinical Infectious Diseases*. https://doi.org/10.1093/CID/CIAA1218

Pan, Y., Li, H., Farmakes, J., Xiao, F., Chen, B., Ma, S., & Yang, Z. (2018). How Do Enzymes Orient When Trapped on Metal-Organic Framework (MOF) Surfaces? *Journal of the American Chemical Society*, *140*(47), 16032–16036. https://doi.org/10.1021/JACS.8B09257/SUPPL_FILE/JA8B09257_SI_001.PDF

Park, J., You, X., Jang, Y., Nam, Y., Kim, M. J., Min, N. K., & Pak, J. J. (2014). ZnO nanorod matrix based electrochemical immunosensors for sensitivity enhanced detection of Legionella pneumophila. *Sensors and Actuators B: Chemical*, *200*, 173–180. https://doi.org/10.1016/J.SNB.2014.03.001

Peruski, A. H., Peruski, L. F., & Jr. (2003). Immunological Methods for Detection and Identification of Infectious Disease and Biological Warfare Agents. *Clinical and Diagnostic Laboratory Immunology*, *10*(4), 506. https://doi.org/10.1128/CDLI.10.4.506-513.2003

Qi, X., Chang, Z., Zhang, D., Binder, K. J., Shen, S., Huang, Y. Y. S., Bai, Y., Wheatley, A. E. H., & Liu, H. (2017). Harnessing surface-functionalized metal-organic frameworks for selective tumor cell capture. *Chemistry of Materials*, *29*(19), 8052–8056. https://doi.org/10.1021/ACS.CHEMMATER.7B03269/SUPPL_FILE/CM7B03269_SI_002.AVI

Ramachandran, D., Brijitta, J., Raj, N. N., Jayanthi, V., & Rabel, A. M. (2013). Synthesis and characterization of Zinc Oxide nanorods. *Proceedings of the International Conference on "Advanced Nanomaterials and Emerging Engineering Technologies", ICANMEET 2013*, 566–568. https://doi.org/10.1109/ICANMEET.2013.6609366

Rapp, B. E., Gruhl, F. J., & Länge, K. (2010). Biosensors with label-free detection designed for diagnostic applications. *Analytical and Bioanalytical Chemistry 2010 398:6*, *398*(6), 2403–2412. https://doi.org/10.1007/S00216-010-3906-2

Reimhult, E., & Höök, F. (2015). Design of Surface Modifications for Nanoscale Sensor Applications. *Sensors (Basel, Switzerland)*, *15*(1), 1635. https://doi.org/10.3390/S150101635

Ricco, R., Pfeiffer, C., Sumida, K., Sumby, C. J., Falcaro, P., Furukawa, S., Champness, N. R., & Doonan, C. J. (2016). Emerging applications of metal–organic frameworks. *CrystEngComm*, *18*(35), 6532–6542. https://doi.org/10.1039/C6CE01030J

Rojas, S., Arenas-Vivo, A., & Horcajada, P. (2019). Metal-organic frameworks: A novel platform for combined advanced therapies. *Coordination Chemistry Reviews*, *388*, 202–226. https://doi.org/10.1016/J.CCR.2019.02.032

Ruiz, G., Tripathi, K., Okyem, S., & Driskell, J. D. (2019). pH Impacts the Orientation of Antibody Adsorbed onto Gold Nanoparticles. *Bioconjugate Chemistry*, *30*(4), 1182–1191. https://doi.org/10.1021/ACS.BIOCONJCHEM.9B00123

Schramm, W., Paek, S. H., & Voss, G. (1993). Strategies for the Immobilization of Antibodies. *ImmunoMethods*, *3*(2), 93–103. https://doi.org/10.1006/IMMU.1993.1043

Segev-Bar, M., & Haick, H. (2013). Flexible Sensors Based on Nanoparticles. *ACS Nano*, *7*(10), 8366–8378. https://doi.org/10.1021/NN402728G

Sharma, S., Byrne, H., & O'Kennedy, R. J. (2016). Antibodies and antibody-derived analytical biosensors. *Essays in Biochemistry*, *60*(1), 9–18. https://doi.org/10.1042/EBC20150002

Sharmin, E., & Zafar, F. (2016). Introductory Chapter: Metal Organic Frameworks (MOFs). *Metal-Organic Frameworks*. https://doi.org/10.5772/64797

Shriver-Lake, L. C., Donner, B., Edelstein, R., Breslin, K., Bhatia, S. K., & Ligler, F. S. (1997). Antibody immobilization using heterobifunctional crosslinkers. *Biosensors and Bioelectronics*, *12*(11), 1101–1106. https://doi.org/10.1016/S0956-5663(97)00070-5

Sibley, C. D., Peirano, G., & Church, D. L. (2012). Molecular methods for pathogen and microbial community detection and characterization: Current and potential application in diagnostic microbiology. *Infection, Genetics and Evolution*, *12*(3), 505–521. https://doi.org/10.1016/J.MEEGID.2012.01.011

Singh, A., & Kashyap, V. K. (2012). Specific and rapid detection of mycobacterium tuberculosis complex in clinical samples by polymerase chain reaction. *Interdisciplinary Perspectives on Infectious Diseases*, *2012*. https://doi.org/10.1155/2012/654694

Subbiah, R., Veerapandian, M., & S. Yun, K. (2011). Nanoparticles: Functionalization and Multifunctional Applications in Biomedical Sciences. *Current Medicinal Chemistry*, *17*(36), 4559–4577. https://doi.org/10.2174/092986710794183024

Sun, C., Hsieh, Y.-P., Ma, S., Geng, S., Cao, Z., Li, L., & Lu, C. (2017). Immunomagnetic separation of tumor initiating cells by screening two surface markers. *Scientific Reports 2017 7:1*, *7*(1), 1–8. https://doi.org/10.1038/srep40632

Sun, X., Du, S., Wang, X., Zhao, W., & Li, Q. (2011). A Label-Free Electrochemical Immunosensor for Carbofuran Detection Based on a Sol-Gel Entrapped Antibody. *Sensors 2011*, *Vol. 11*, *Pages 9520-9531*, *11*(10), 9520–9531. https://doi.org/10.3390/S111009520

Taheri, R. A., Rezayan, A. H., Rahimi, F., Mohammadnejad, J., & Kamali, M. (2016). Comparison of antibody immobilization strategies in detection of Vibrio cholerae by surface plasmon resonance. *Biointerphases*, *11*(4), 041006. https://doi.org/10.1116/1.4971270

Teulon, J.-M., Delcuze, Y., Odorico, M., Chen, S. W., Parot, P., & Pellequer, J.-L. (2011). Single and multiple bonds in (strept)avidin–biotin interactions. *Journal of Molecular Recognition*, *24*(3), 490–502. https://doi.org/10.1002/JMR.1109

Trilling, A. K., Beekwilder, J., & Zuilhof, H. (2013). Antibody orientation on biosensor surfaces: a minireview. *Analyst*, *138*(6), 1619–1627. https://doi.org/10.1039/C2AN36787D

Ugelstad, J., Stenstad, P., Kilaas, L., Prestvik, W., Herje, R., Berge, A., & Hornes, E. (1993). Monodisperse magnetic polymer particles. New biochemical and biomedical applications. *Blood Purification*, *11*(6), 349–369. https://doi.org/10.1159/000170129

Ulman, A. (1996). Formation and Structure of Self-Assembled Monolayers. *Chemical Reviews*, *96*(4), 1533–1554. https://doi.org/10.1021/CR9502357

Um, H. J., Kim, M., Lee, S. H., Min, J., Kim, H., Choi, Y. W., & Kim, Y. H. (2011). Electrochemically oriented immobilization of antibody on poly-(2-cyano-ethylpyrrole)-coated gold electrode using a cyclic voltammetry. *Talanta*, *84*(2), 330–334. https://doi.org/10.1016/J.TALANTA.2011.01.013

VanGuilder, H. D., Vrana, K. E., & Freeman, W. M. (2018). Twenty-five years of quantitative PCR for gene expression analysis. *Https://Doi.Org/10.2144/000112776*, *44*(5), 619–626. https://doi.org/10.2144/000112776

Varlet-Marie, E., Sterkers, Y., Perrotte, M., & Bastien, P. (2018). A new LAMP-based assay for the molecular diagnosis of toxoplasmosis: comparison with a proficient PCR assay. *International Journal for Parasitology*, *48*(6), 457–462. https://doi.org/10.1016/J.IJPARA.2017.11.005

Vashist, S. K., & Luong, J. H. T. (2018). Antibody Immobilization and Surface Functionalization Chemistries for Immunodiagnostics. *Handbook of Immunoassay Technologies: Approaches, Performances, and Applications*, 19–46. https://doi.org/10.1016/B978-0-12-811762-0.00002-5

Velásquez-Hernández, M. de J., Linares-Moreau, M., Astria, E., Carraro, F., Alyami, M. Z., Khashab, N. M., Sumby, C. J., Doonan, C. J., & Falcaro, P. (2021). Towards applications of bioentities@MOFs in biomedicine. *Coordination Chemistry Reviews*, *429*, 213651. https://doi.org/10.1016/J.CCR.2020.213651

Vestergaard, M., Kerman, K., & Tamiya, E. (2007). An Overview of Label-free Electrochemical Protein Sensors. *Sensors 2007, Vol. 7, Pages 3442-3458*, *7*(12), 3442–3458. https://doi.org/10.3390/S7123442

Vouga, M., & Greub, G. (2016). Emerging bacterial pathogens: the past and beyond. *Clinical Microbiology and Infection*, *22*(1), 12–21. https://doi.org/10.1016/J.CMI.2015.10.010

Wadell, G., Varsànyi, T. M., Lord, A., & Sutton, R. N. P. (1980). EPIDEMIC OUTBREAKS OF ADENOVIRUS 7 WITH SPECIAL REFERENCE TO THE PATHOGENICITY OF ADENOVIRUS GENOME TYPE 7b. *American Journal of Epidemiology*, *112*(5), 619–628. https://doi.org/10.1093/OXFORDJOURNALS.AJE.A113034

Wahid, B., Ali, A., Rafique, S., & Idrees, M. (2016). Zika: As an emergent epidemic. *Asian Pacific Journal of Tropical Medicine*, *9*(8), 723–729. https://doi.org/10.1016/J.APJTM.2016.06.019

Wang, C., Wang, L., Tadepalli, S., Morrissey, J. J., Kharasch, E. D., Naik, R. R., & Singamaneni, S. (2018). Ultrarobust Biochips with Metal-Organic Framework Coating for Point-of-Care Diagnosis. *ACS Sensors*, *3*(2), 342–351. https://doi.org/10.1021/acssensors.7b00762

Wang, H., & Ma, Z. (2019). "Off-on" signal amplification strategy amperometric immunosensor for ultrasensitive detection of tumour marker. *Biosensors and Bioelectronics*, *132*(December 2018), 265–270. https://doi.org/10.1016/j.bios.2019.03.013

Wang, Y., Xu, H., Zhang, J., & Li, G. (2008). Electrochemical Sensors for Clinic Analysis. *Sensors 2008, Vol. 8, Pages 2043-2081*, *8*(4), 2043–2081. https://doi.org/10.3390/S8042043

Wang, Z., & Cohen, S. M. (2009). Postsynthetic modification of metal–organic frameworks. *Chemical Society Reviews*, *38*(5), 1315–1329. https://doi.org/10.1039/B802258P

Warsinke, A., Benkert, A., & Scheller, F. W. (2000). Electrochemical immunoassays. *Fresenius' Journal of Analytical Chemistry 2000 366:6*, *366*(6), 622–634. https://doi.org/10.1007/S002160051557

Welch, N. G., Scoble, J. A., Muir, B. W., & Pigram, P. J. (2017). Orientation and characterization of immobilized antibodies for improved immunoassays (Review). *Biointerphases*, *12*(2), 02D301. https://doi.org/10.1116/1.4978435

Wencel, D., Abel, T., & McDonagh, C. (2013). Optical Chemical pH Sensors. *Analytical Chemistry*, *86*(1), 15–29. https://doi.org/10.1021/AC4035168

West, R., & Kobokovich, A. (2020). *Understanding the Accuracy of Diagnostic and Serology Tests: Sensitivity and Specificity Factsheet*.

Wijaya, E., Lenaerts, C., Maricot, S., Hastanin, J., Habraken, S., Vilcot, J. P., Boukherroub, R., & Szunerits, S. (2011). Surface plasmon resonance-based biosensors: From the development of different SPR structures to novel surface functionalization strategies. *Current Opinion in Solid State and Materials Science*, *15*(5), 208–224. https://doi.org/10.1016/j.cossms.2011.05.001

World Health Organization. (2015, December 10). *WHO publishes list of top emerging diseases likely to cause major epidemics*. https://www.who.int/news/item/10-12-2015-who-publishes-list-of-top-emerging-diseases-likely-to-cause-major-epidemics

Xia, J., Tong, J., Liu, M., Shen, Y., & Guo, D. (2020). Evaluation of coronavirus in tears and conjunctival secretions of patients with SARS-CoV-2 infection. *Journal of Medical Virology*, *92*(6), 589–594. https://doi.org/10.1002/JMV.25725

Yang, S., & Rothman, R. E. (2004). PCR-based diagnostics for infectious diseases: uses, limitations, and future applications in acute-care settings. *The Lancet Infectious Diseases*, *4*(6), 337–348. https://doi.org/10.1016/S1473-3099(04)01044-8

Yetisen, A. K., Akram, M. S., & Lowe, C. R. (2013). Paper-based microfluidic point-of-care diagnostic devices. *Lab on a Chip*, *13*(12), 2210–2251. https://doi.org/10.1039/C3LC50169H

Yim, C., Lee, H., Lee, S., & Jeon, S. (2017). One-step immobilization of antibodies on ZIF-8/Fe3O4 hybrid nanoparticles for the immunoassay of Staphylococcus aureus. *RSC Advances*, *7*(3), 1418–1422. https://doi.org/10.1039/C6RA25527B

Zauli, D. A. G. (2019). PCR and Infectious Diseases. *Synthetic Biology - New Interdisciplinary Science*. https://doi.org/10.5772/INTECHOPEN.85630

Zea, M., Bellagambi, F. G., Ben Halima, H., Zine, N., Jaffrezic-Renault, N., Villa, R., Gabriel, G., & Errachid, A. (2020). Electrochemical sensors for cortisol detections: Almost there. *TrAC - Trends in Analytical Chemistry*, *132*, 116058. https://doi.org/10.1016/j.trac.2020.116058

Zhan, W., Kuang, Q., Zhou, J., Kong, X., Xie, Z., & Zheng, L. (2013). Semiconductor@Metal–Organic Framework Core–Shell Heterostructures: A Case of ZnO@ZIF-8 Nanorods with Selective Photoelectrochemical Response. *Journal of the American Chemical Society*, *135*(5), 1926–1933. https://doi.org/10.1021/JA311085E

Zhang, J., Tan, Y., & Song, W. J. (2020). Zeolitic imidazolate frameworks for use in electrochemical and optical chemical sensing and biosensing: a review. *Microchimica Acta*, *187*(4). https://doi.org/10.1007/s00604-020-4173-3

Zhang, W., Besford, Q. A., Christofferson, A. J., Charchar, P., Richardson, J. J., Elbourne, A., Kempe, K., Hagemeyer, C. E., Field, M. R., McConville, C. F., Yarovsky, I., & Caruso, F. (2020). Cobalt-Directed Assembly of Antibodies onto Metal-Phenolic Networks for Enhanced Particle Targeting. *Nano Letters*, *20*(4), 2660–2666. https://doi.org/10.1021/ACS.NANOLETT.0C00295

Zhang, Y., Zhang, Z., Rong, S., Yu, H., Gao, H., Ding, P., Chang, D., & Pan, H. (2020). Electrochemical immunoassay for the carcinoembryonic antigen based on Au NPs modified zeolitic imidazolate framework and ordered mesoporous carbon. *Microchimica Acta*, *187*(5). https://doi.org/10.1007/s00604-020-04235-5

Zuk, R., Ginsberg, V., Houts, T., Rabbie, J., Merrick, H., Ullman, E. F., Fischer, M., Sizto, C. C., Stiso, S. N., & Litman, D. J. (1985). Enzyme immunochromatography--a quantitative immunoassay requiring no instrumentation. *Clinical Chemistry*, *31*(7), 1144–1150. https://pubmed.ncbi.nlm.nih.gov/3891138/